

Review

Hierarchical Structure–Ferroelectricity Relationships of Barium Titanate Particles

Tu Lee* and Ilhan A. Aksay

Department of Chemical Engineering and Princeton Materials Institute,
Princeton University, Princeton, New Jersey 08544-5211

Received May 3, 2001

ABSTRACT: The aim of this paper is to dissect the hierarchical structures of BaTiO₃ particles into primary, secondary, tertiary, and quaternary structural levels and to thoroughly review the corresponding structure–ferroelectricity relationships at all levels. This analytical framework is of growing importance for the fundamental understanding of the ferroelectric properties of BaTiO₃ in microelectronic devices, especially as their structural levels are all approaching the same scale in the process of miniaturization. The identification of the most influential structure among others and the deduction of a meaningful structure–ferroelectricity relationship depend on a thorough understanding of the relationships.

1. Introduction

Since the discovery of BaTiO₃ by Wainer and Salomon in 1942,¹ the fundamentals of its ferroelectricity have often been related to its tertiary structure (ferroelectric domains) by assuming both primary (ionic spacing) and secondary (crystal lattice) structures are perfect (Table 1). Structural features of the ferroelectric domains and their dependence on control parameters such as pressure (compressive stress), p , electric fields, E , and temperature, T , have been well-studied in a bulk BaTiO₃ crystal. Correspondingly, the cooperative effect of these domains, which is reflected in ferroelectric properties such as polarization, P , and lattice strain, x , have been accounted for by the phenomenological theory of Devonshire in 1949.²

Although Slater's local field theory in 1950³ had shown the important role that the primary and secondary structures play in ferroelectricity, Devonshire's surface-modified phenomenological theory has been widely used to explain the *size effect* of BaTiO₃ particles from a quaternary structural point of view. The BaTiO₃ particle is often thought to contain two portions: a ferroelectric core covered with a paraelectric layer (core–shell model). However, the inconsistency of the critical size in the literature, ranging from 15 to 200 nm in diameter,^{4–26} suggests that the ferroelectric

Table 1. Structure–Ferroelectricity Relationships of BaTiO₃

level	structure	structure–ferroelectricity relationship
primary	perfect ionic spacing	Slater local field
primary	impurities	random field
secondary	perfect crystal lattice	Slater local field
secondary	lattice defects	random field theory
tertiary	ferroelectric domains	Devonshire phenomenological
quaternary	particle size (core–shell)	surface modified Devonshire

properties of BaTiO₃ particles should not be a function of the quaternary structure (Euclidean geometry) alone. There is actually a need to reconsider the contribution from the lower structural levels.

The aim of this paper is to review all of the above-mentioned structure–ferroelectricity relationships at different structural levels and to introduce the random field theory to account for the dependence of ferroelectricity on lattice defects occurring in primary and secondary structures in BaTiO₃ powders (Table 1). This is of growing importance for a fundamental understanding of the ferroelectric properties of BaTiO₃ in microelectronic devices, as their structural levels are all approaching the same scale in the process of miniaturization. The identification of the most influential structure among others and the deduction of a meaningful structure–ferroelectricity relationship depend on a thorough understanding of the relationships. Additionally, the analytical framework of dissecting BaTiO₃ particles into structures at different levels in this paper

* To whom correspondence should be addressed at Bristol-Myers Squibb Pharmaceutical Research Institute, One Squibb Drive, P.O. Box 191, New Brunswick, NJ 08903-0191. E-mail: tu.lee@bms.com.

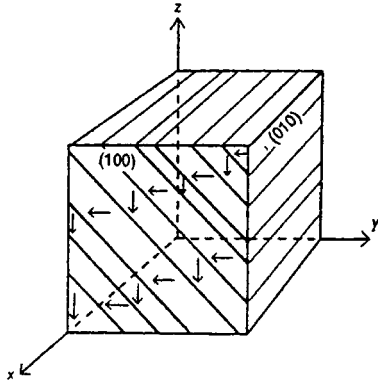


Figure 1. Diagram of simply twinned crystals of BaTiO₃ showing the twin boundaries. Short arrows indicate the *c* direction of the individual components.³³

may be extended to other related hierarchical structures, such as BaTiO₃ grains and thin films, to reconcile the contradiction in the effects of grain size^{27–30} and the inconsistency of the effects of thickness,³¹ respectively.

2. Ferroelectric Domains

There are two kinds of ferroelectric domains, 90 and 180°. They are mechanical twins associated with the tetragonal phase occurring about the {101} and {100} planes, respectively. The domains are produced by phase transitions as the mechanism for the strain release and by the depolarization field as the reduction of electrostatic energy.^{32–34} The 90° walls are all {101} planes. They are the boundaries of two domains that are polarized at 90° to each other. The 180° walls are all {100} planes, and they are the boundaries between domains with antiparallel polarization.³⁵

Although the internal symmetry of the BaTiO₃ crystal is tetragonal at room temperature, it is a composite of ferroelectric domains separated by the twin boundaries.³³ Only a very small number of truly single BaTiO₃ crystals are observed, invariably in the form of very thin flakes or needles. X-ray photographs of such crystals oscillated about any cube axis show a repeat distance of ~4.0 Å. Since $a = 3.9932 \pm 0.0002$ Å and $c = 4.0341 \pm 0.0003$ Å, this indicates that all the component twins lie with *c* axes parallel to one of the cube axes of the crystal.³³ A BaTiO₃ crystal exhibiting complex twinning is shown in Figure 1.³³ In contrast to the (111) twins, ferroelectric twins may easily be changed through local heating of a thin section with an electron beam in an electronic microscope.³²

2.1. Domain Wall Thickness. The wall thickness, N , may be calculated from the minimum of the total wall energy density, σ_w , with respect to N . σ_w is the sum of the dipole–dipole interaction, σ_{dip} , and the contribution from the anisotropy, σ_{anis} ³⁵

$$\frac{\partial \sigma_w}{\partial N} = \frac{\partial (\sigma_{\text{dip}} + \sigma_{\text{anis}})}{\partial N} = \frac{\partial \left[\left(\frac{10^{-14}}{Na^2} \right) + \left(\frac{1}{2} C_{33} Z_Z^2 Na \right) \right]}{\partial N} = 0 \quad (1)$$

where C_{33} = elastic constant, Z_Z = the spontaneous

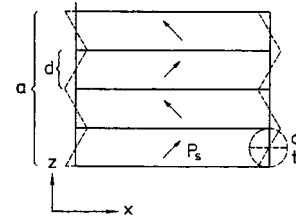


Figure 2. Cubic-shaped grain split into 90° domains, embedded in an isotropic dielectric medium. If the grain is free (not clamped), it is distorted, as shown by dashed lines. The circle indicates the region of elastic energy in the upper half with compressive stress, *c*, and in the lower half with tensile stress, *t*.²⁹

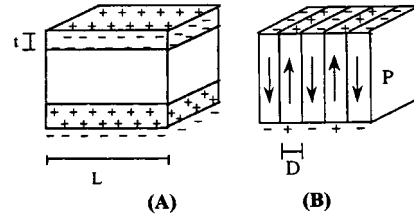


Figure 3. (A) Space-charge layer having a thickness of *t* with uniform charge distribution. (B) Cubic crystal of size *L* with domains of alternating polarization separated by 180° domain walls. The domain width is *D*.³⁶

strain at room temperature, and a = lattice constant. N becomes³⁵

$$N \cong \left(\frac{2 \times 10^{-14}}{C_{33} Z_Z^2 a^3} \right)^{1/2} \approx 1 \quad (2)$$

This indicates that the wall thickness in BaTiO₃ is extremely small, on the order of 1 to a very few lattice constants.

2.2. Domain Size. The domain size in ferroelectric materials is a state of equilibrium between the energy of the domain walls and the energies of those electric and elastic fields, which are caused by spontaneous polarization and strain.³⁴

Artl, Hennings, and de With²⁹ approximated the equilibrium size of the 90° domain, d , by the minimum in the sum mainly of the domain wall energy and the mechanical field energy. They assumed that the multidomain BaTiO₃ crystal is clamped by its surroundings so that it cannot expand freely (Figure 2). They obtain

$$d = \left[\frac{128\pi g \sigma}{C_{11} S_S^2} \right]^{1/2} \approx 0.8 \mu\text{m} \quad (3)$$

with the spontaneous strain,³⁴ S_S , during the cubic-to-tetragonal transition

$$S_S = (1 - a/c) \quad (4)$$

where a and c = lattice constants, C_{11} = average longitudinal elastic constant, g = crystal size, and σ = domain wall energy.

On the other hand, Shih and Aksay³⁶ assumed that the multidomain BaTiO₃ crystal is stress-free and only took the depolarization energy and the space-charge layers into account (Figure 3) and estimated the equilibrium size of the 180° domain, D , by the minimization

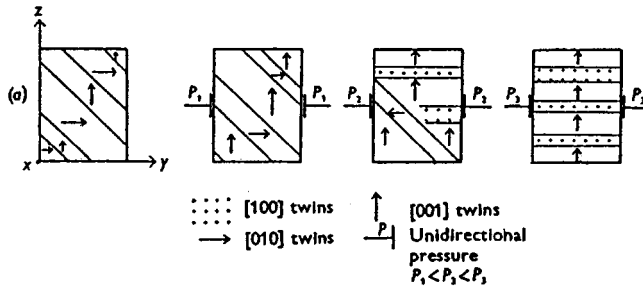


Figure 4. Diagrams (from left to right) showing the effect of unidirectional pressure on BaTiO₃ crystals.³³

of the free energy density $F(P, D, L)$ with respect to D . They obtained

$$D = \left[\frac{\gamma}{1.7P^2} \right]^{1/2} L^{1/2} \left[\frac{L}{t} \right]^{1/2} \approx 0.1 \mu\text{m} \quad (5)$$

with D = the 180° domain width, γ = domain wall energy, P = polarization, L = the size of the crystal, and t = space-charge layer thickness ranging from 10² to 10⁴ Å.

3. Control Parameters

The crystallographic directions of ferroelectric domains may be altered by three parameters: pressure, electric fields, and temperature.

3.1. Pressure. If a unidirectional pressure is applied along the y axis of a well-formed crystal, the [001] and [100] twins grow in volume at the expense of the [010] twins by a migration of the twin boundaries in a direction perpendicular to their own plane. The boundaries become progressively less numerous until the whole crystal is a composite of [001] and [100] twins only (Figure 4).³³

A pressure (compressive stress) may only rotate the polar direction by 90°, and it results in a large strain.³⁷ Domain walls grow as spikes^{35,37} or wedges.^{33,38} If a spike is taken to be a lamina with thickness w and length L , the minimum stress, σ^0 , needed to induce 90° domain spikes under compressive stress is³⁷

$$\sigma^0 = \frac{2\Gamma_{90}}{w\gamma_S} \quad (6)$$

where Γ_{90} = the 90° domain wall energy and γ_S = spontaneous strain. The forward velocity, V , induced by the stress field, σ , is³⁷

$$V = M \left(\gamma_S \sigma - \frac{2\Gamma_{90}}{w} \right) \quad (7)$$

with M = the domain wall mobility = 4.8×10^{-4} m³/s N.

As the temperature of the crystal is increased, it becomes more susceptible to applied pressures. Above the Curie temperature, T_C , when the crystal is normally isotropic (cubic), small pressures will make it anisotropic (tetragonal). Therefore, it should be possible to produce single crystals from twinned crystals by simultaneous pressure along the x and y directions, especially if the

crystals are at the same time cooled slowly through the Curie temperature.³³

Samara³⁹ has shown that the inverse proportionality between T_C and pressure, p , suggests that the unidirectional pressure should decrease the T_C value of a single BaTiO₃ crystal (instead of raising it as Kay alleged originally³³). The inverse relationship of T_C and p has been verified by experiments and by the negative value of the cubic–tetragonal phase transition volume change, ΔV , in the Clausius–Clapeyron equation^{39,40}

$$\frac{\partial T_C}{\partial p} = \frac{\Delta V}{\Delta S} = \frac{T_C \Delta V}{Q} \quad (8)$$

with ΔS = the entropy change, Q = cubic–tetragonal phase transition latent heat, and $\Delta V = -0.062$ Å³/unit cell. Consequently, pressure favors the smaller volume, a stabilization of the cubic phase, or a decrease in T_C .

3.2. Electric Fields. If electric fields are applied along the y direction between opposite cube faces of a well-formed crystal, [001] twins grow in volume at the expense of the [100] and [010] twins by a migration of the twin boundaries in a direction perpendicular to their own plane.³³ Unlike the effect of a unidirectional pressure, an electric field may rotate the polar direction by either 90 or 180°. A 180° polar rotation does not result in any strain.³⁷

The minimum electric fields, E_{90}^0 and E_{180}^0 , needed to drive 90 and 180° domain spikes are³⁷

$$E_{90}^0 = \frac{2\Gamma_{90}}{P_S w} \quad (9)$$

$$E_{180}^0 = \frac{\Gamma_{180}}{P_S w} \quad (10)$$

with Γ_{90} = 90° domain wall energy, Γ_{180} = 180° domain wall energy, P_S = spontaneous polarization, and w = domain thickness. The forward velocities, V_{90} and V_{180} , of 90 and 180° domain spikes induced by the electric fields, E_{90}^0 and E_{180}^0 , are

$$V_{180} = M \left(2P_S E_{180}^0 - \frac{2\Gamma_{180}}{w} \right) \quad (11)$$

$$V_{90} = M \left(P_S E_{90}^0 - \frac{2\Gamma_{90}}{w} \right) \quad (12)$$

with M = the domain wall mobility = 4.8×10^{-4} m³/s N.

The stronger the field, the more effective the aligning process is. A complete saturation may be obtained in the case of a twinned crystal. This may result in a single domain crystal whose c axis becomes completely oriented in a direction parallel to the applied field, and all the twin boundaries disappear. The voltage required for saturation depends on the complexity of the specimen and the time of application of the field. A typical value is around 15 000 V/cm.³³ When the field is completely reduced to zero, the crystal may remain perfectly single if complete saturation was previously achieved, but more often partial relaxation of the orientation occurs, although the crystal never returns completely to its original twin configuration.³³ Slow relaxation of the crystal can be achieved by keeping it in a closed

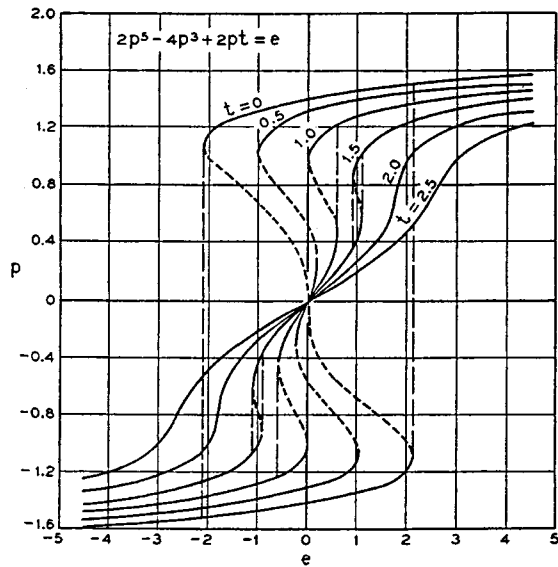


Figure 5. Plot of the function $2p^5 - 4p^3 + 2pt = e$.⁴²

electrical circuit.^{33,36,41} In addition, slow reversal of the field usually allows some [001] twins to appear. Increasing the frequency to 50 cycles/s renders the crystal much more opaque, owing to the decrease in domain size and the increase of relative proportion of boundary material. The boundaries are seen to be in a state of violent agitation. The stress involved with high voltages often crack the crystal in an irregular way, which does not obviously conform to single crystallographic directions.³³

The application of a strong field, E , raises the Curie temperature⁴², T_C , in accordance with a linear relationship⁴⁰

$$\frac{\partial T_C}{\partial E} = -\frac{\Delta P}{\Delta S} = \frac{T_C P_{SC}}{Q} \quad (13)$$

with ΔS = the entropy change, Q = cubic–tetragonal phase transition latent heat, and ΔP = the discontinuous jump of the spontaneous polarization, P_S , at T_C upon heating ($= 0 - P_{SC} = -P_{SC}$).

Consequently, Merz⁴² has observed that at temperatures higher than T_C ($> T_2$), the cubic crystal is paraelectric (nonferroelectric) and the P – E plot gives a straight line, where $T_2 = T_C + 11.7$ °C.⁴³ At lower temperatures, ($T_C > T > T_2$), the material can be driven to the ferroelectric state when a strong enough field, E_{CRIT} , is applied, which gives a double-hysteresis P – E loop. At temperatures near T_C , however, these two loops overlap. The temperature dependence of the P – E plot is shown in Figure 5.⁴² Using thermodynamics, the phenomenological representation of the P – E plot as a function of temperature can be expressed as⁴²

$$e = 2p^5 + 4p^3 + 2pt \quad (14)$$

where

$$p = (3C/B)^{1/2} P \quad (15)$$

$$e = (27C^3/B^5)^{1/2} E \quad (16)$$

$$t = (3\beta C/B^2)(T - T_0) \quad (17)$$

with P = electrical polarization; β , B , and C = constants,

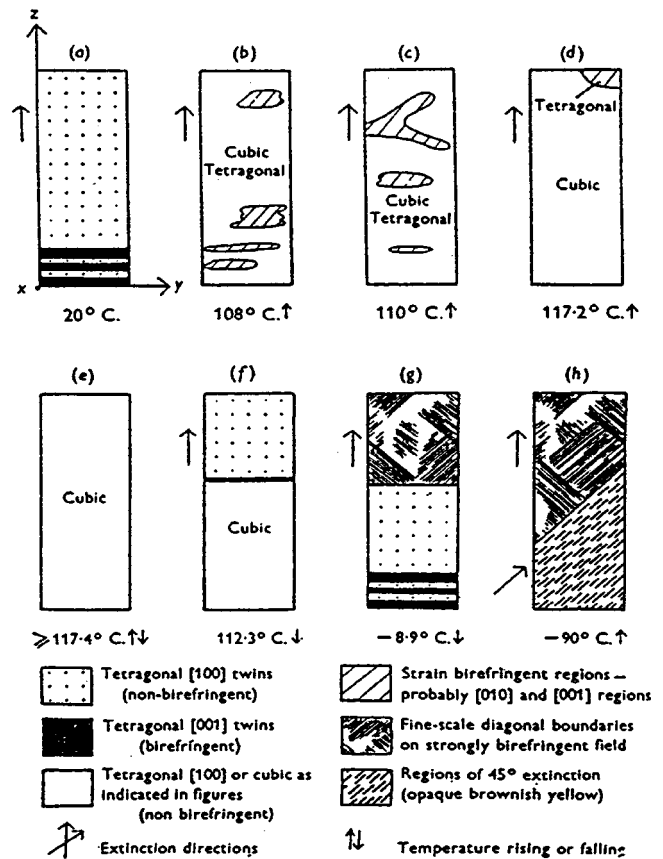


Figure 6. Appearance in a thin plate of BaTiO₃ at different temperatures.³³

and T_0 = extrapolated temperature of the reciprocal dielectric constant plot of $1/\epsilon(T)$, where $T_0 \cong T_C - 7.7$ °C.⁴³ The plot of eq 14 is shown in Figure 5.⁴²

In general, P_S can be obtained by extrapolation of the P – E curve back to the E_{CRIT} ordinate.⁴⁰ Since the P – E plot is a straight line at temperatures $> T_2$, $P_S = 0$ regardless of the strength of the applied field. At lower temperatures, $T_C > T > T_2$, P_S decreases as E_{CRIT} increases. At T_C , $P_S = P_{SC}$ and $E_{CRIT} = 0$. Figure 5 shows that, once below T_C , P_S increases (with $E_{CRIT} = 0$) as T decreases. We will discuss the P – E plot in greater details in section 4.

3.3. Temperature. Kay³³ has found, as shown in Figure 6,³³ that as the BaTiO₃ crystal plate is slowly heated near the T_C , the twin boundaries often become slightly curved. They no longer conform exactly to simple crystallographic directions. The small amounts of [001] tetragonal twins have the a -cell dimensions parallel to the thinnest dimension of the plate and are able to expand as T_C is approached. However, the large [100] twins have both a and b cell dimensions in the plane of the crystal plate, and the necessity for their expansion opposes the tetragonal–cubic transition. This will result in stress restricting the transition of neighboring portions of the [100] tetragonal component. Some of the boundaries begin to migrate irregularly through the crystal. This explains the temperature range of the tetragonal–cubic transition from 108 to 117.5 °C. This also results in the reorientation from [100] to [010] and [001] directions. These patches with “dislocations” or “faults” become smaller and fainter and eventually disappear, leaving the crystal completely isotropic (cubic) at T_C .

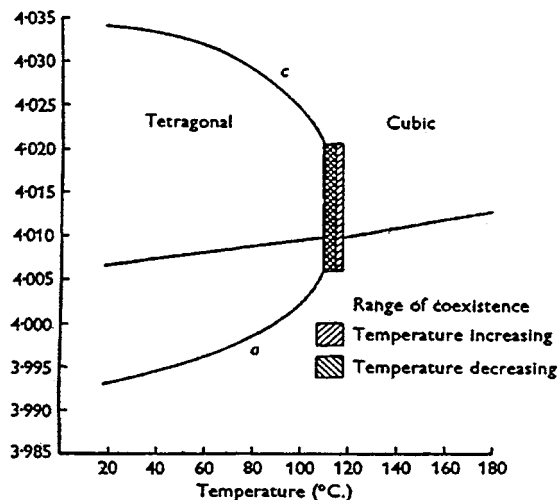


Figure 7. Relation between cell parameters and temperature for a single crystal of BaTiO₃. The cube root of the cell volume is shown for the tetragonal phase. The tetragonal and cubic phases coexist in the shaded region.³³

When it is cooled, the crystal returns to a composite of tetragonal twins whose arrangement usually varies after each cycle. The more rapid the cooling is, the greater the complexity will be. Slow cooling alone, however, has rarely produced truly single tetragonal crystals. This is probably due to strain centers resulting from local lattice imperfections characteristic of each individual crystal. Since the decrease in temperature and the strain effects tend to cooperate and produce the anisotropic (tetragonal) phase, the temperature range of the cubic–tetragonal transition should be less than the case of raising temperature. It is found to be from 114.8 to 109.8 °C.

The value of d/a , as determined by the X-ray diffraction, decreases as the temperature increases due to the contraction of c and the expansion of a ($b = a$) near the tetragonal–cubic phase transition. The relation between cell parameters and temperature for a single BaTiO₃ crystal is demonstrated in Figure 7.³³ At the transition, T_C , the tetragonal parameters are $a = 4.0051 \pm 0.0008$ Å and $c = 4.0206 \pm 0.0007$ Å and the cubic parameter is $a = 4.0096 \pm 0.0002$ Å ($a = b = c$). It should be noted that the T_C value of crystal BaTiO₃ is different from that usually stated for powder materials, as shown in Figure 8.⁹ This may result, for example, either from compositional differences^{44,45} or from the intense strain effects inherent in polycrystalline aggregates produced by the powder-sintering process.^{29,46}

4. Ferroelectric Properties and Devonshire's Theory

There are five main ferroelectric properties of BaTiO₃: (i) the ferroelectric polarization–electric field (P – E) loop for a multidomain BaTiO₃ crystal, (ii) polarization of BaTiO₃ as a function of temperature for a single-domain BaTiO₃ crystal (P – T curve), (iii) the temperature dependence of dielectric constants for small fields of a single-domain BaTiO₃ crystal (ϵ – T plot), (iv) the temperature dependence of the spontaneous strain for a single-domain BaTiO₃ crystal (unit cell parameters

vs T plot), and (v) the stress dependence of the dielectric constant for fine grained BaTiO₃ ceramics (ϵ – σ curve). All these experimental observations can be interpreted by a thermodynamic model, namely, the phenomenological theory of Devonshire.² This approach, however, is a purely macroscopic and does not describe the atomic displacements, which accompany the process of polarization and the switching of a ferroelectric. Also, it is only valid for the equilibrium properties and does not apply to nonequilibrium conditions, which occur, for example, during the switching of a ferroelectric.⁴³

The standard procedure of Devonshire's theory is to expand the free energy function in terms of certain independent variables, such as polarization and stress, to use certain measured properties of the crystal to determine coefficients, and then to predict other properties. It is always possible to describe the experimental results by adding as many terms to the expansion as necessary. The difficult point, however, is to explain the experimental facts with the smallest number of expansion coefficients possible and on the basis of the most reasonable assumptions.⁴⁰

4.1. Polarization vs Electric Field (P – E Loop).

BaTiO₃ crystals are generally comprised of multiple ferroelectric twins. The consequences are manifested in the characteristic hysteresis P – E loop. The ferroelectric hysteresis loops can be directly observed on a cathode ray oscilloscope,^{35,40,42,47} and the hysteresis loop is shown schematically in Figure 9.⁴⁰

Consider the simplest case of a crystal below T_C with electrodes perpendicular to the polar axis and consisting of an equal number of positive and negative domains. The domains are antiparallel with respect to some given crystallographic direction so that only the inversion of 180° domains is involved. When the electric field, E , is increased in the positive direction, the positive domains grow with an average velocity³⁵ of the order of $(1-5) \times 10^4$ cm/s and at the expense of the negative domains. The polarization, P , increases very rapidly (OA) (Figure 9) and reaches a saturation value (BC) when all domains are aligned in the direction of the field. This means that now the crystal has a "single domain" structure. When the field is reduced to zero again, a few domains remain aligned. At zero applied field, $E = E_{CRIT} = 0$, and below T_C , a finite value of the polarization can be measured, called the remnant polarization, P_r (OD). Extrapolation of the linear portion BC of the hysteresis loop back to the polarization axis, where $E = E_{CRIT} = 0$, yields the value of the spontaneous polarization, P_s (OE). It corresponds to the saturation polarization with all dipoles aligned in parallel.⁴⁸ To annihilate the remnant polarization, P_r , we must apply an electric field in the opposite (negative) direction. The field needed for this purpose is called the coercive field, E_c (OF). Upon further increase in the field in the negative direction, uniform alignment of the dipoles can again be achieved, this time in the direction opposite to the previous one (GH).

The temperature dependence of hysteresis loops is demonstrated in Figure 5 and described by eqs 14–17.

Merz⁴² has used the phenomenological theory proposed by Devonshire² to explain the general characteristics of the ferroelectric hysteresis loop. The differential dU of the internal energy of a body subject to external

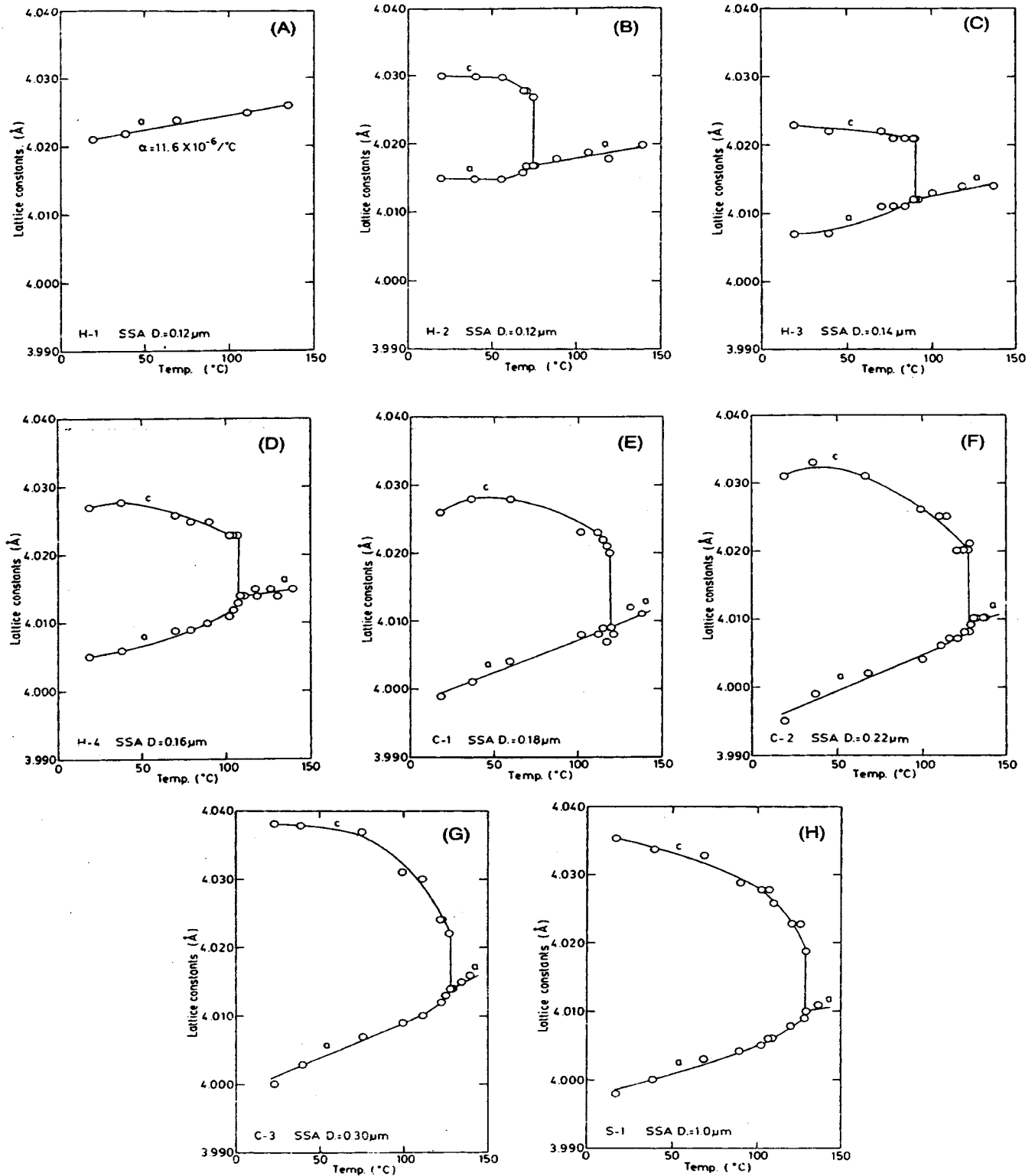


Figure 8. Change in lattice constants with temperature (heating run): (A) hy, virgin, $D = 0.12 \mu\text{m}$; (B) hy, at 400°C , $D = 0.12 \mu\text{m}$; (C) hy, at 600°C , $D = 0.14 \mu\text{m}$; (D) hy, at 800°C , $D = 0.16 \mu\text{m}$; (E) co, at 900°C , $D = 0.18 \mu\text{m}$; (F) co, at 1000°C , $D = 0.22 \mu\text{m}$; (G) co, at 1050°C , $D = 0.30 \mu\text{m}$; (H) ss, at 1100°C , $D = 1.0 \mu\text{m}$.⁹ Particles are prepared by three processes, hydrothermal (hy), coprecipitation (co), and solid-state reaction (ss), and their diameters, D , are grown to a larger size by firing.

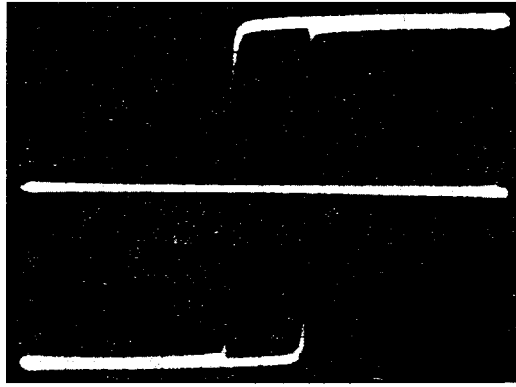
stress and electric fields is⁴³

$$dU = TdS - \sum_{i=1}^3 X_i dx_i + \vec{E} \cdot d\vec{P} \quad (18)$$

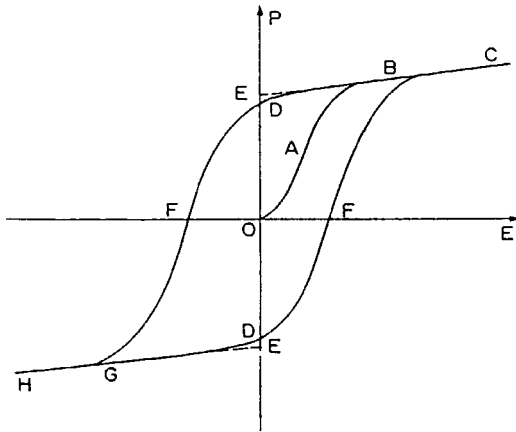
where S = entropy, T = temperature, x_i = strain, X_i =

stress components, \vec{E} = electric field, and \vec{P} = polarization. Since the elastic Gibbs function is⁴³

$$G = U + \sum_i X_i x_i - TS \quad (19)$$



(A)



(B)

Figure 9. (A) Hysteresis loop of a good BaTiO₃ single crystal at 60 cps. (B) Ferroelectric hysteresis loop (schematic). OE = spontaneous polarization P_s ; OF = coercive field strength E_c .⁴⁰

hence, as follows from eq 19

$$dG = -SdT + \sum_{i=1}^3 x_i dX_i + \bar{E} \cdot d\bar{P} \quad (20)$$

Assuming the stress, X_i , to be constant, we can expand G in powers of the polarization, P , where the coefficients are functions of temperature⁴³

$$G = \beta(T - T_0)(P_x^2 + P_y^2 + P_z^2) - B(P_x^4 + P_y^4 + P_z^4) + C(P_x^6 + P_y^6 + P_z^6) + D(P_y^2 P_z^2 + P_z^2 P_x^2 + P_x^2 P_y^2) + \dots + G_0(T) \quad (21)$$

Terms in odd powers of the polarization components are omitted because we want the free energy function to be the same for reversal of the signs of any of the polarization components.⁴⁰ The first coefficient, $\beta(T - T_0)$, is a linear function of temperature. Its significance and the constants β and T_0 will be explained in section 4.3. The second coefficient of eq 21, $-B$, is negative, and it describes BaTiO₃ with a phase transition of the first order, which is distinguished by a discontinuous change of the saturation polarization at the transition temperature (see section 4.2). If the polar axis is aligned with

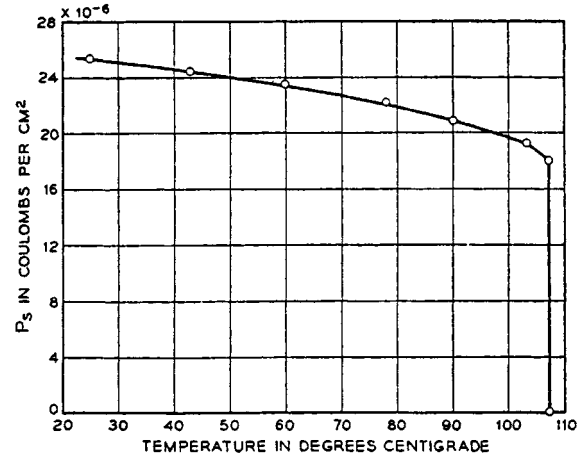


Figure 10. Spontaneous electrical polarization P_s vs temperature T .⁴²

electric fields along the z direction, we have $P_x = 0$, $P_y = 0$, and $P_z = P$. Equation 21 is simplified to⁴³

$$G = \beta(T - T_0)P^2 - BP^4 + CP^6 + G_0 \quad (22)$$

where G_0 , the free energy for zero polarization, is often equated to zero.⁴³ Differentiating eq 22 with respect to P gives the following equation for the electric field, E , acting on a ferroelectric, in terms of the polarization, P

$$\frac{\partial G}{\partial P} = E = 2\beta(T - T_0)P - 4BP^3 + 6CP^5 \quad (23)$$

The nonlinear relationship of the E - T plot can be expressed by eq 23, which can be simplified to eqs 14-17.⁴²

4.2. Polarization vs Temperature Curve (P - T Curve). Below T_C , the regular hysteresis loop is obtained as shown in Figure 9. The value of the spontaneous polarization, P_s , can be determined by measuring the distance OE, where $E = E_{\text{CRIT}} = 0$, on the observed loop on a calibrated screen of the cathode ray tube.⁴² It is also possible, of course, to determine the temperature dependence of the spontaneous polarization, P_s , of the ferroelectric crystal, by observing the change of the distance OE as a function of the temperature of the crystal. Near T_C , the hysteresis loop splits into two smaller loops because the crystal becomes ferroelectric only when under the influence of a high electric field.⁴² P_s is now obtained by extrapolation of the linear portion of the hysteresis loop back to the ordinate axis, where $E = E_{\text{CRIT}} \neq 0$. At higher temperatures, the double-hysteresis loop collapses into a straight line passing through the origin. The crystal is paraelectric, and at no part of the cycle is the electric field high enough to shift T_C enough to make it ferroelectric.⁴² P_s is equal to 0 regardless of the magnitude of E . The P - T plot is illustrated in Figure 10.⁴²

The T_C value and the corresponding value P_{SC} of the spontaneous polarization can be calculated from eq 22 by imposing that the free energy of the polar phase, G , and the nonpolar phase, G_0 , are equal, which leads to⁴³

$$G - G_0 = \beta(T_C - T_0)P_{\text{SC}}^2 - BP_{\text{SC}}^4 + CP_{\text{SC}}^6 = 0 \quad (24)$$

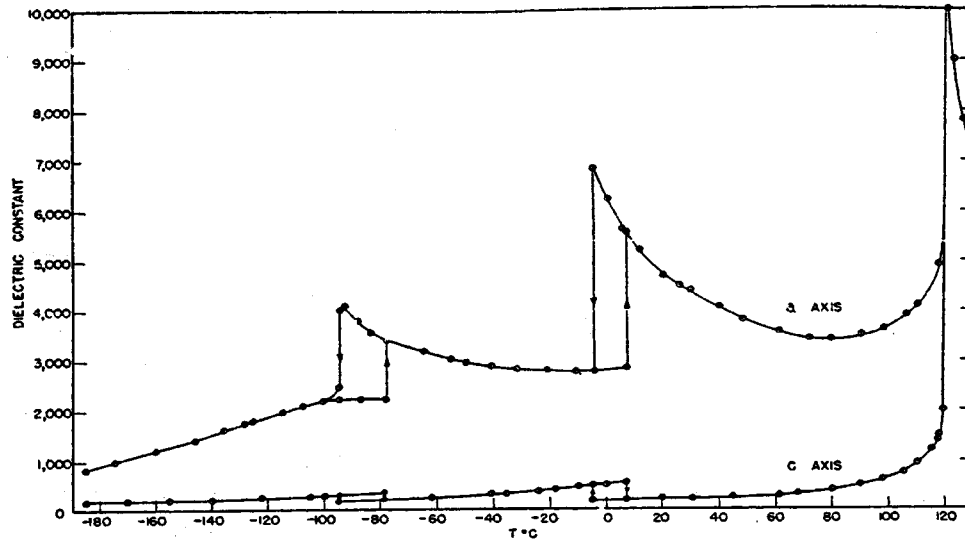


Figure 11. Dielectric constants ϵ_a and ϵ_c as a function of temperature.⁴⁷

Near T_C , P_S can still occur with $E = E_{\text{CRIT}} = 0$ and eq 23 becomes⁴³

$$\frac{\partial G}{\partial P} = E = 2\beta(T_C - T_0)P_{\text{SC}} - 4BP_{\text{SC}}^3 + 6CP_{\text{SC}}^5 = 0 \quad (25)$$

P_{SC}^2 and T_C can be obtained by solving eqs 24 and 25⁴³

$$P_{\text{SC}}^2 = -\frac{(-B)}{2C} \quad (26)$$

$$T_C = T_0 + \frac{B^2}{4\beta C} \quad (27)$$

For BaTiO_3 , $P_{\text{SC}} = 17.5 \mu\text{C}/\text{cm}^2$ and $T_C = T_0 + 7.7 \text{ }^\circ\text{C}$.⁴³

For P_{SC}^2 to be real in eq 26, the coefficient of the P^4 term has to be negative: that is, $-B$. It describes a ferroelectric with a transition of the first order in which the change from the ferroelectric to the paraelectric state is accompanied by a discontinuous change⁴⁹ of the saturation polarization P_S at T_C , namely P_{SC} .

The three portions of the P - T plot: the cubic (paraelectric) state, the phase transition, and the tetragonal (ferroelectric) state, may be represented by the following equations.²

For a cubic state ($> T_C$)

$$P_x = P_y = P_z = 0 \quad (28)$$

At the phase transition ($\sim T_C$)

$$P_x = P_y = 0 \quad (29)$$

$$P = P_z = P_{\text{SC}} \quad (30)$$

For a tetragonal phase ($< T_C$)

$$P_x = P_y = 0 \quad (31)$$

and

$$\frac{\partial^2 G}{\partial P_z^2} = 2\beta(T - T_0) - 12BP_z^2 + 30CP_z^4 = 0 \quad (32)$$

where $P_z = P$. As the temperature, T , falls, the magnitude of the polarization, P , increases. This is well demonstrated by Figure 10.⁴²

4.3. Dielectric Constant vs Temperature (ϵ - T Plot). Well above T_C , in the paraelectric state, the relation between polarization, P , and field, E , is linear;⁴² therefore, the dielectric constant is field-independent.² In the ferroelectric region, however, the existence of a hysteresis loop clearly demonstrates that the value of the dielectric constant depends on the field strength with which it is measured. If the applied field, E , is very small, no new domains are created, and no movement of the domain boundaries takes place. In this case, one measures the dielectric constant of the crystal with no interference from the domain structure. This quantity, which is called the initial dielectric constant,⁴⁰ is directly proportional to the slope of the virgin curve OA in Figure 9B at the zero point. It is this constant to which we refer when we speak of the dielectric constant, ϵ , of a ferroelectric crystal.

When a crystal plate is cooled below T_C , it normally shows a rather complicated domain structure. Measurement with a small, applied field perpendicular to the major surfaces would furnish an average dielectric constant whose value would depend on the relative ratio between numbers of c domains and a domains. To avoid this confusion, Merz selected, at room temperature, a single-domain plate grown by Remeika's method⁵⁰ with the c axis perpendicular to the major surfaces for the measurement of ϵ_c ; for the measurement of ϵ_a , he selected a single-domain plate with the c axis in the major surfaces.⁴⁰ Figure 11 gives the plot of the dielectric constants ϵ_a and ϵ_c as functions of temperature determined by Merz.⁴⁷

In the high-temperature region above T_C , where the crystal has cubic symmetry, the dielectric constant, ϵ , is independent of direction^{40,47}

$$\epsilon = \epsilon_a = \epsilon_c \quad (33)$$

The dielectric constant of an isotropic or cubic medium

relative to vacuum is defined in terms of the macroscopic field,⁴⁹ E

$$\epsilon = \frac{\epsilon_0 E + P}{\epsilon_0 E} = 1 + \chi = 1 + \frac{1}{\chi'} \quad (34)$$

where

$$\chi = \frac{1}{\chi'} = \frac{P}{\epsilon_0 E} \quad (35)$$

with ϵ_0 = the permittivity (dielectric constant) of a vacuum, χ = the susceptibility at constant stress X , and χ' = the reciprocal susceptibility at constant stress X .

Since χ' is also defined by

$$\chi' = \frac{\partial E}{\partial P} \quad (36)$$

and at high temperatures above T_C the polarization, P , in eq 23 becomes very small, χ' can hence be approximated as⁴³

$$\chi' \approx \frac{\partial E}{\partial P} \approx 2\beta(T - T_0) \quad (37)$$

In accordance with eqs 34 and 37, the dielectric constant, ϵ , is linearly related to the slope of the P - E loop

$$\epsilon \approx \frac{\partial P}{\partial E} \approx \frac{1}{2\beta(T - T_0)} \quad (38)$$

or

$$\frac{1}{\epsilon} \approx 2\beta(T - T_0) \quad (39)$$

Equation 39 is the Curie–Weiss law, valid in the cubic paraelectric region, where the P - E curve becomes a straight line with a slope,⁴² which can be approximated as a function of temperature, T .⁴³ The Curie constant, 2β , can be determined by the slope of the $1/\epsilon$ vs T plot, and the Curie–Weiss temperature, T_0 , can be assessed accurately by extrapolating the linear dependence to the T axis.^{42,51}

However, in the temperature regions below T_C , where the tetragonal crystal has less symmetry, the dielectric constant is no longer independent of direction. Also, the relation between field and polarization is no longer linear.² To generalize the calculations, we will apply the same convention to both cubic and tetragonal phases. Since ϵ is related to χ' by eq 34, and χ' is defined as

$$\chi'_r = \frac{\partial E}{\partial P_r} = \frac{\partial^2 G}{\partial P_r^2} \quad (40)$$

where $r = x, y$, and z directions. From eqs 21, 34, and 40, the two regions of the ϵ - T plot can be represented by eqs 42, 44, and 45. For the cubic phase²

$$P_x = P_y = P_z = P = 0 \quad (41)$$

$$\chi'_r = \chi'_y = \chi'_z = 2\beta(T - T_0) \approx \frac{1}{\epsilon} \quad (42)$$

Equation 37 becomes eq 42 when $T > T_C$. For the

tetragonal phase²

$$P_x = P_y = 0 \quad (43)$$

$$\chi'_x = \chi'_y = 2\beta(T - T_0) + 2DP_z^2 \approx \frac{1}{\epsilon_a} \quad (44)$$

$$\chi'_z = 2\beta(T - T_0) - 12BP_z^2 + 30CP_z^4 \approx \frac{1}{\epsilon_c} \quad (45)$$

Above T_C , in the cubic structure, the Ti^{4+} ions oscillate about the centers of the TiO_6 octahedra without effective mutual coupling, but with large dipole moments, because the Ti^{4+} ion has a tendency to change from ionic to covalent bonding as its distance to an atom decreases.³⁷ At T_C , both ionic and electronic polarizability reach peak levels, and the dielectric constant ($\epsilon = \epsilon_c = \epsilon_a$) reaches a very high value of about 10 000.^{47,52} Harwood et al.⁵³ attributed the peak to a finite time transition between the cubic and tetragonal phases, resulting in instantaneous permittivities corresponding to those of the separate phases at temperatures at which they would not exist or would already be admixed with the other phase. Below T_C , the interaction between dipoles overcomes the thermal agitation. The high polarizability of the O^{2-} ions results in the highly charged Ti^{4+} ions taking up a mean position closer to one of the O^{2-} ions in each octahedron. The Ti^{4+} ions are locked in an eccentric position displaced toward one of the six oxygen neighbors.³⁸ Within small volumes, domains and all the Ti^{4+} ions are displaced in the same direction, resulting in the formation of a polar c axis and converting the structure from cubic to tetragonal. Thus, for two out of the six O^{2-} ions, the electronic and ionic polarizabilities are reduced by the interaction with Ti^{4+} ions. As a consequence, the dielectric constant in the polar c direction, ϵ_c , is on the order of a few hundreds at room temperature and is much smaller than the dielectric constant in the a direction, ϵ_a , which on the order of several thousands. This also means that ions and electrons are easier to move in the a direction perpendicular to the polarization under an electric field.^{38,40} Using Merz's crystal, Matthias and von Hippel³⁸ have also constructed similar plots of dielectric constant vs T in the (100), (010), and (001) directions.

4.4. Unit Cell Parameters vs Temperature (c - or a - T Plot). The ionic displacements also result in a change in lattice dimensions. This is demonstrated in Figure 12.⁵⁴ Above T_C , the BaTiO_3 crystal has a simple cubic array of corner-sharing TiO_6 octahedra with barium ions filling the holes between them.⁵² At the cubic–tetragonal transition near T_C , there is an expansion in the direction of the Ti^{4+} displacements and a contraction in perpendicular directions. The cubic parameter is $a = b = c = 4.0096 \pm 0.0002$ Å, and the tetragonal parameters are $a = b = 4.0051 \pm 0.0008$ Å and $c = 4.0206 \pm 0.0007$ Å.³³ The atomic displacements are oscillations about a nonpolar site; after a displacive transition,⁵² the oscillations are about a polar site.⁴⁹ Since there are six possible equilibrium positions for the Ti^{4+} ion in each TiO_6 octahedron to shift to, if there are N unit cells in the crystal, statistically, there would be the large number of 6^N possible polar complexions.⁵²

To study the strain which accompanies spontaneous polarization, Devonshire² expressed the Helmholtz free

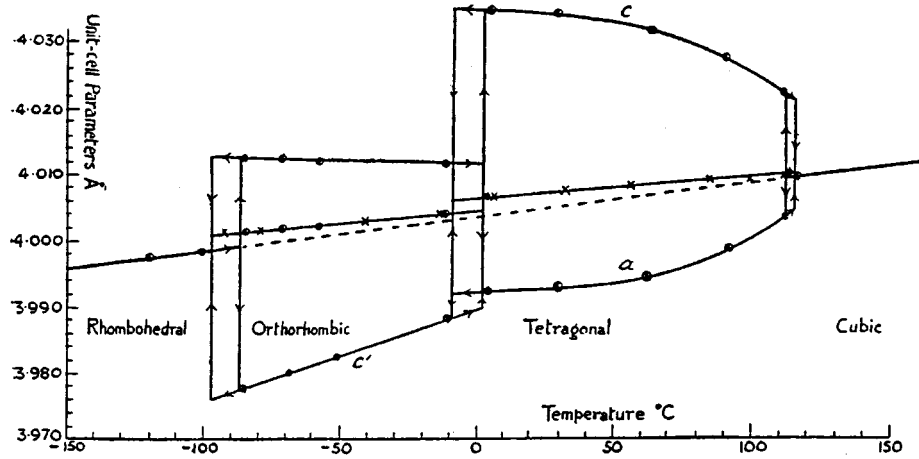


Figure 12. Variation of cell parameters with temperature in BaTiO₃ crystals.⁵⁴

energy, A , as a function of strain, x_i , and polarization, P . Since

$$dA = dU - TdS - SdT \quad (46)$$

Substituting eq 18 into eq 46, eq 47 becomes

$$dA = -SdT - \sum_{i=1}^3 X_i dx_i + \vec{E} \cdot d\vec{P} \quad (47)$$

$$A = \frac{1}{2}c_{11}(x_x^2 + y_y^2 + z_z^2) + c_{12}(y_y z_z + z_z x_x + x_x y_y) + \frac{1}{2}c_{44}(x_x^2 + y_y^2 + z_z^2) + \beta(T - T_0)(P_x^2 + P_y^2 + P_z^2) - B(P_x^4 + P_y^4 + P_z^4) + C(P_y^2 P_z^2 + P_z^2 P_x^2 + P_x^2 P_y^2) + g_{11}(x_x P_x^2 + y_y P_y^2 + z_z P_z^2) + g_{12}\{x_x(P_y^2 + P_z^2) + y_y(P_z^2 + P_x^2) + z_z(P_x^2 + P_y^2)\} + g_{44}(y_z P_y P_z + z_x P_z P_x + x_y P_x P_y) + \dots + A_0(T) \quad (48)$$

Let $A_0(T)$, the free energy of the unpolarized cubic crystal, be zero. Also, the components of the stress are given by the equation

$$X_i = \frac{\partial A}{\partial x_i} \quad (49)$$

By assuming the three components of stress, X_x , X_y , and X_z , to be zero, three relations between strain and polarization are obtained. Solving these equations for the strain in terms of the polarization gives

$$x_x = y_y = P_z^2 \frac{g_{11}c_{12} - g_{12}c_{11}}{(c_{11} - c_{12})(c_{11} + 2c_{12})} \quad (50)$$

$$z_z = P_z^2 \frac{-g_{11}(c_{11} + c_{12}) + 2g_{12}c_{12}}{(c_{11} - c_{12})(c_{11} + 2c_{12})} \quad (51)$$

For a cubic phase, $P_z = 0$, and eqs 50 and 51 become

$$x_x = y_y = z_z = 0 \quad (52)$$

Therefore, the temperature dependence of the cubic lattice³ is purely due to the volume coefficient of expansion of 3×10^{-5} unit. For a tetragonal phase, P_z

is aligned with the electric field along the z direction; thus, eqs 50 and 51 apply. Since P_z is a function of T according to eq 32, and the strains are⁴⁰

$$x = \frac{\Delta a}{a} \quad y = \frac{\Delta b}{b} \quad z = \frac{\Delta c}{c} \quad (53)$$

with a , b , and c being the lattice parameters and Δ the change, the unit cell parameters vs T plot can now be represented by eqs 50–53.

4.5. Dielectric Constant vs Stress (ϵ - σ Curve).

Buessem, Cross, and Gaswami²⁷ proposed that the internal stress in fine-grained materials must be greater than that in coarse-grained ceramics because, as the grain size decreases, the grain size becomes comparable with the domain wall thickness so that the number of the stress-relieving 90° domains decreases. Under this condition, grain boundaries would contribute additional pinning points for the moving walls. The internal stress in fine-grained materials is believed to give rise to a high dielectric constant. This view is verified by using Devonshire's phenomenological theory² as applied to ferroelectrics in eq 21. The free energy of the system was expanded in terms of polarization and the electrostrictive coupling terms between stress and polarization

$$G_1 - G_{10} = -\frac{1}{2}s_{11}(X_x^2 + Y_y^2 + Z_z^2) - s_{12}(X_x Y_y + Y_y Z_z + Z_z X_x) - \frac{1}{2}s_{44}(X_y^2 + Y_z^2 + Z_x^2) + (Q_{11}X_x + Q_{12}Y_y + Q_{12}Z_z)P_x^2 + (Q_{12}X_x + Q_{11}Y_y + Q_{12}Z_z)P_y^2 + (Q_{12}X_x + Q_{12}Y_y + Q_{11}Z_z)P_z^2 + Q_{44}(X_y P_x P_y + Y_z P_y P_z + Z_x P_z P_x) + A(P_x^2 + P_y^2 + P_z^2) + B(P_x^4 + P_y^4 + P_z^4) + C(P_x^6 + P_y^6 + P_z^6) + D(P_x^2 P_y^2 + P_y^2 P_z^2 + P_z^2 P_x^2) + G(P_x^2 P_y^4 + P_x^4 P_y^2 + P_y^2 P_z^4 + P_y^4 P_z^2 + P_z^2 P_x^4 + P_z^4 P_x^2) \quad (54)$$

where X_x , Y_y , and Z_z = normal stress components, X_y , Y_z , and Z_x = shear stress components, s_{11} , s_{12} , and s_{44} = elastic compliances, P_x , P_y , and P_z = components of polarization, Q_{11} , Q_{12} , and Q_{44} = electrostrictive coef-

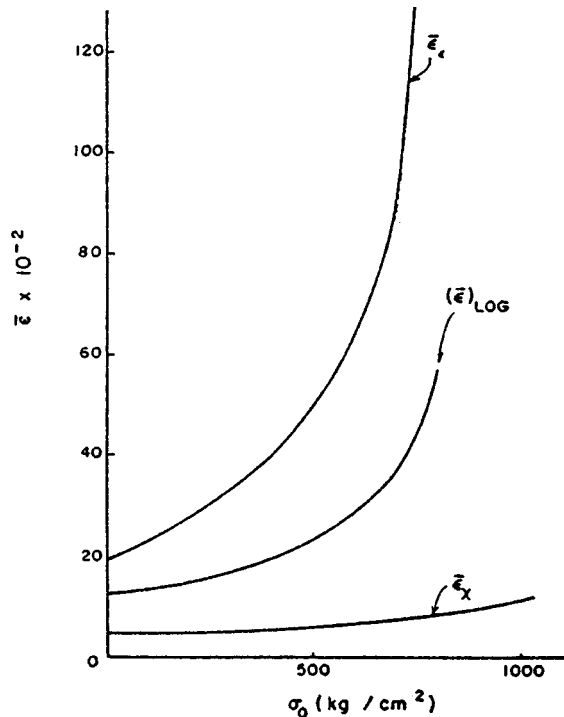


Figure 13. Variation of average permittivity with stress for fine-grained barium titanate.²⁷

ficients, and $A, B, C, D,$ and $G =$ coefficients of free energy function. The dielectric constant expressions were given by

$$\frac{1}{\epsilon_0 \epsilon_a} = \frac{1}{\epsilon_0 \epsilon_{xx}} = \frac{\partial^2 G_1}{\partial P_x^2} \quad (55)$$

$$\frac{1}{\epsilon_0 \epsilon_c} = \frac{1}{\epsilon_0 \epsilon_{zz}} = \frac{\partial^2 G_1}{\partial P_z^2} \quad (56)$$

For spontaneous polarization

$$E = 0 = \frac{\partial G}{\partial P} \quad P_x = P_y = 0 \quad P_z = P_s \quad (57)$$

From eq 57, P_z can be solved for any given values of stresses. With this P_z and for the same stress values, the dielectric constant may be calculated from eqs 55 and 56. This is illustrated in Figure 13.²⁷

Samara³⁹ observed that, for single BaTiO_3 crystals, the dielectric constant in the immediate vicinity of the peak increased by 50–60% under 15 kbar of pressure (Figure 14). However, for the ceramic sample, it decreased by over 50% for the same pressure range (Figure 14). He related this striking difference to the pressure dependence of the dielectric constant along the a axis, which had not been measured. For the single crystals, ϵ was measured along the c axis. Since this axis decreased with pressure at a faster rate than the a axis, pressure might switch some c domains to a domains and increase the number of a domains along the c direction, thus leading to a higher ϵ_c (lower ϵ_a). In ceramics, of course, it was the average value of ϵ that was measured.

5. Local Field Theory

Although Devonshire's phenomenological theory^{2,43} has been very useful in describing the essence of

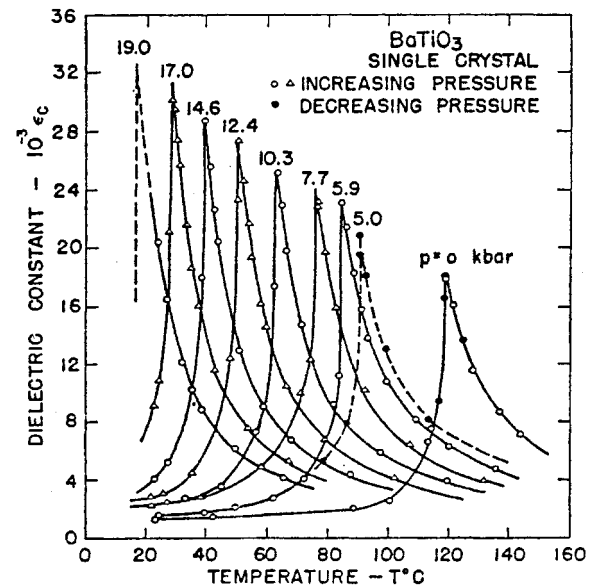


Figure 14. Temperature dependence of the dielectric constant of single-crystal BaTiO_3 measured along the c axis at various hydrostatic pressures.³⁹

ferroelectricity through the correlation of the free energy of a ferroelectric crystal, G , as a function of polarization, P , with "macroscopic parameters" of $\beta(T - T_0)$, $-B, C, D,$ and $G_0(T)$

$$G = \beta(T - T_0)(P_x^2 + P_y^2 + P_z^2) - B(P_x^4 + P_y^4 + P_z^4) + C(P_x^6 + P_y^6 + P_z^6) + D(P_y^2 P_z^2 + P_z^2 P_x^2 + P_x^2 P_y^2) + \dots + G_0(T) \quad (21)$$

atomic model theory is needed to link the macroscopic parameters with the microscopic structures. Slater's local field theory^{3,55} provides the connection by computing the exact local Lorentz field, not assuming spherical symmetry but taking account of the precise crystal structure.

The value of the local field that acts at the site of the atom, E_{local} , is related to the value of the macroscopic electric field, E , by⁴⁹

$$E_{\text{local}} = E + E_2 + E_3 \quad (58)$$

where

$$E = E_0 + E_1 \quad (59)$$

where $E_0 =$ field produced by fixed charges external to the body, $E_1 =$ depolarization field from a surface charge density $\mathbf{n} \cdot \mathbf{P}$ on the outer surface of the specimen (electrodes), $E_2 =$ Lorentz cavity field (field from polarization charges on the inside of a spherical cavity cut (as a mathematical fiction) out of the specimen with the reference atom as center), and $E_3 =$ field of atoms inside the spherical cavity.

For a spherical cavity,⁴⁹ the Lorentz cavity field, E_2 , is $P/3\epsilon_0$, where $P =$ the polarization and $\epsilon_0 =$ permittivity. $E_3 = 0$ when the elementary particles are neutral without permanent dipole moments or when they are arranged either in complete disorder or in cubic or

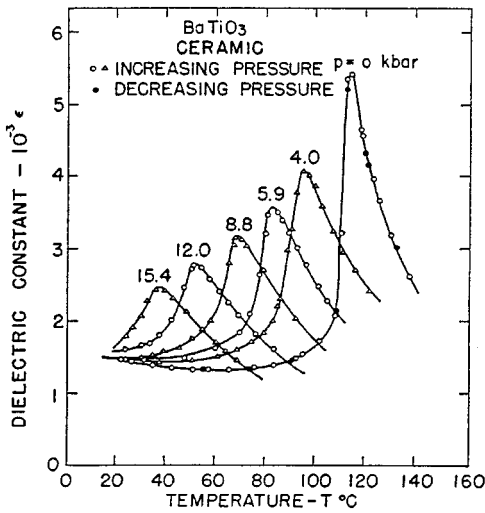


Figure 15. Temperature dependence of the dielectric constant of pure ceramic BaTiO₃ at various hydrostatic pressures.³⁹

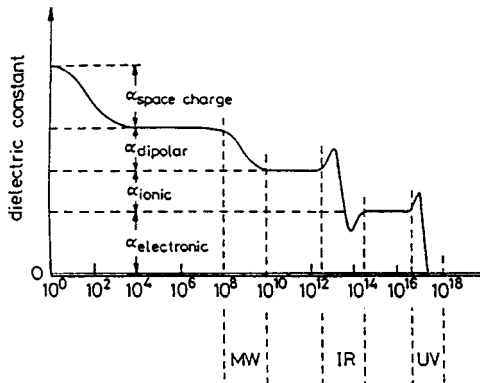


Figure 16. Frequency response of the dielectric constant.⁵⁷

similar highly symmetrical arrays.⁵⁶ Equation 58 becomes

$$E_{\text{local}} = E + \frac{P}{3\epsilon_0} \quad (60)$$

This is the Lorentz relation that bridges the local property to the macroscopic property.

The polarization of a crystal may be expressed approximately as the product of the polarizabilities, α , of the atoms times the local electric field, E_{local}

$$P = N\alpha E_{\text{local}} = N\alpha \left(E + \frac{P}{3\epsilon_0} \right) = \frac{\alpha}{v} \left(E + \frac{P}{3\epsilon_0} \right) \quad (61)$$

where N = number of atoms per unit volume = $1/v$ with v = the volume of a unit cell. The polarizability, α , is an atomic property^{49,56,57}

$$\alpha = \alpha_e + \alpha_i + \alpha_d + \alpha_s \quad (62)$$

with α_e = electronic polarizability, α_i = ionic polarizability, α_d = dipolar polarizability and α_s = space charge polarizability. They are related to the frequency of the external field as shown in Figure 16.⁵⁷

The dielectric constant, ϵ , is defined as the ratio of the permittivity constant of a dielectric material, ϵ' , to the permittivity of a free space,⁴⁸ ϵ_0

$$\epsilon = \frac{\epsilon'}{\epsilon_0} \quad (63)$$

$$\epsilon' E = \epsilon_0 E + P \quad (64)$$

where the total electric flux through a dielectric material, $\epsilon' E$, is the sum of the electric field through free space, $\epsilon_0 E$, and dipole charge, P . Equations 63 and 64 can be rearranged into eq 34. Equation 64 gives the definition of polarization.

Using eq 61 to find an expression of P/E and substituting that into eq 34, we get the Clausius–Mossotti equation³

$$\epsilon = 1 + \frac{P}{\epsilon_0 E} = 1 + \frac{\frac{\alpha}{\epsilon_0 v}}{1 - \frac{1}{3} \frac{\alpha}{\epsilon_0 v}} \quad (65)$$

The dielectric constant, ϵ , must approach infinity when the polarizability term of the denominator, $\alpha/\epsilon_0 v$, approaches 1. Obviously, this is bound to happen at a critical or Curie temperature T_0 , when permanent dipole moments, μ , contribute a dipole (orientation) polarizability, α_d

$$\alpha_d = \frac{\mu^2}{3kT} \quad (66)$$

This equation is based on several assumptions.⁵⁸ Molecules carrying a permanent dipole moment suffer a torque in an electric field that tends to align the dipole axis in the field direction. Thermal agitation, on the other hand, tends to maintain a random distribution. The outcome of these counteracting influences is a Boltzmann statistical equilibrium that can be calculated without reference to the actual rotation of the molecules and their interaction as long as the electric field changes so slowly that the equilibrium is reached with certainty.

Forgetting about the deformation polarization, we may replace α by α_d in eq 66 and obtain⁵⁹

$$\epsilon = 1 + \frac{3T_0}{T - T_0} \quad (67)$$

where

$$T_0 = \frac{\mu^2}{9\epsilon_0 v k} \quad (68)$$

Equation 67 is the famous Curie–Weiss law of ferromagnetism, here derived for permanent electric instead of magnetic dipole moments. It predicts the spontaneous polarization (or magnetization) of dielectrics containing such moments.

Actually, a Mosotti-type catastrophe ($\alpha/\epsilon_0 v = 3$) happens only under very special conditions. The reason is that permanent electric dipole moments are anchored in molecular groups that tend to lose their freedom of orientation in condensed phases through association and steric hindrance. Even if these groups could rotate like

spheres in a medium of high friction, the Clausius–Mosotti formula would not apply, since the reference molecule in the spherical cavity is not a mathematical point but is itself a dipole carrier. As soon as the cavity is visualized as a molecular sphere in which a mathematical dipole is centered, calculations carried through by Onsager⁶⁰ show that spontaneous polarization does not occur.

In Osager's treatment, the surroundings of the dipole are still considered as a continuum. An improved model of Kirkwood⁶¹ visualizes the dipole molecule with its first layer of neighbors as a structural unit, known in its statistical arrangement from X-ray patterns. The behavior of such a molecular island, floating in a dielectric continuum, is examined for static fields; the permittivities thus found are in fair agreement with experiment. To obtain still better results, the molecular island is extended to include the second nearest neighbors, but the mathematical problem becomes increasingly formidable.

Although eqs 65 and 67 are primitive, their general forms are sacrosanct in the field of ferroelectricity in describing the ferroelectric behavior. Theories have been developed to modify and to relate them to the microscopic structures of ferroelectrics. In Slater's local field theory,³ α is treated as $\alpha_e + \alpha_i$ in eq 70, the Lorentz factor of $1/3$ is substituted by $-C_4/C_3$ in eq 71 based on the exact lattice structure of BaTiO₃, and α is determined to be a function of temperature, T , in eq 88.

Since each unit cell in the BaTiO₃ crystal contains five ions, Slater³ proposed that the local field, E_{local} , in eq 60 should be modified to the local fields exerted at the position of each ion, by the lattices of the dipoles of all types of ions

$$\begin{aligned}
 E_{\text{local}}^{\text{Ti}} &= E + \left(\frac{1}{\epsilon_0}\right) \left[\frac{1}{3}P_{\text{Ti}} + \frac{1}{3}P_{\text{Ba}} + \left(q + \frac{1}{3}\right)P_{\text{O}_a} + \right. \\
 &\quad \left. \left(-\frac{1}{2}q + \frac{1}{3}\right)(P_{\text{O}_{b1}} + P_{\text{O}_{b2}}) \right] \\
 E_{\text{local}}^{\text{Ba}} &= E + \left(\frac{1}{\epsilon_0}\right) \left[\frac{1}{3}P_{\text{Ti}} + \frac{1}{3}P_{\text{Ba}} + \left(-p + \frac{1}{3}\right)P_{\text{O}_a} + \right. \\
 &\quad \left. \left(\frac{1}{2}p + \frac{1}{3}\right)(P_{\text{O}_{b1}} + P_{\text{O}_{b2}}) \right] \\
 E_{\text{local}}^{\text{O}_a} &= E + \left(\frac{1}{\epsilon_0}\right) \left[\left(q + \frac{1}{3}\right)P_{\text{Ti}} + \left(-p + \frac{1}{3}\right)P_{\text{Ba}} + \frac{1}{3}P_{\text{O}_a} + \right. \\
 &\quad \left. \left(\frac{1}{2}p + \frac{1}{3}\right)(P_{\text{O}_{b1}} + P_{\text{O}_{b2}}) \right] \\
 E_{\text{local}}^{\text{O}_{b1}} &= E + \left(\frac{1}{\epsilon_0}\right) \left[\left(-\frac{1}{2}q + \frac{1}{3}\right)P_{\text{Ti}} + \left(\frac{1}{2}p + \frac{1}{3}\right)P_{\text{Ba}} + \right. \\
 &\quad \left. \left(\frac{1}{2}p + \frac{1}{3}\right)P_{\text{O}_a} + \frac{1}{3}P_{\text{O}_{b1}} + \left(-p + \frac{1}{3}\right)P_{\text{O}_{b2}} \right] \\
 E_{\text{local}}^{\text{O}_{b2}} &= E + \left(\frac{1}{\epsilon_0}\right) \left[\left(-\frac{1}{2}q + \frac{1}{3}\right)P_{\text{Ti}} + \left(\frac{1}{2}p + \frac{1}{3}\right)P_{\text{Ba}} + \right. \\
 &\quad \left. \left(\frac{1}{2}p + \frac{1}{3}\right)P_{\text{O}_a} + \left(-p + \frac{1}{3}\right)P_{\text{O}_{b1}} + \frac{1}{3}P_{\text{O}_{b2}} \right] \quad (69)
 \end{aligned}$$

with O_a = type a oxygen atoms that lie along the same line of the polarization axis, O_{b1} and O_{b2} = the two type b oxygen atoms that are at the right angles to the polarization axis, $p = 0.690$, and $q = 2.394$. The values

of p and q are related to the local field exerted at various points through the lattice by a lattice of dipoles whose polarization is unity, polarized along the z direction. Similarly, eq 61 becomes

$$\begin{aligned}
 P_{\text{Ti}} &= \left(\frac{\alpha_{\text{Ti}} + \alpha'_{\text{Ti}}}{\nu}\right) E_{\text{local}}^{\text{Ti}} \\
 P_{\text{Ba}} &= \left(\frac{\alpha_{\text{Ba}}}{\nu}\right) E_{\text{local}}^{\text{Ba}} \\
 P_{\text{O}_a} &= \left(\frac{\alpha_{\text{O}_a}}{\nu}\right) E_{\text{local}}^{\text{O}_a} \\
 P_{\text{O}_{b1}} &= \left(\frac{\alpha_{\text{O}_{b1}}}{\nu}\right) E_{\text{local}}^{\text{O}_{b1}} \\
 P_{\text{O}_{b2}} &= \left(\frac{\alpha_{\text{O}_{b2}}}{\nu}\right) E_{\text{local}}^{\text{O}_{b2}} \quad (70)
 \end{aligned}$$

where α = electronic polarization and α' = ionic polarization. Combining eqs 69 and 70 to get a total P/E , substituting it into eq 34, and letting $X_j = \alpha_j/\epsilon_0\nu$ and $X'_j = \alpha'_j/\epsilon_0\nu$ for species j , the Lorentz correction for the dielectric constant, ϵ , becomes

$$\epsilon = 1 + \frac{c_1 + c_2 X'_{\text{Ti}}}{c_3 + c_4 X'_{\text{Ti}}} = 1 + \frac{c_2}{c_4} + \frac{\frac{c_1}{c_3} - \frac{c_2}{c_4}}{1 + \frac{c_4}{c_3} X'_{\text{Ti}}} \quad (71)$$

where

$$\begin{aligned}
 c_1 &= X_{\text{Ti}} + X_{\text{Ba}} + 3X_{\text{O}} + pX_{\text{Ti}}X_{\text{O}} + 3pX_{\text{O}}^2 - \\
 &\quad \left(\frac{3}{2}\right)(p + q)^2 X_{\text{Ti}}X_{\text{Ba}}X_{\text{O}} - \frac{1}{2}(3q - p)^2 X_{\text{Ti}}X_{\text{O}}^2 - 8p^2 X_{\text{Ba}}X_{\text{O}}^2 \\
 c_2 &= 1 + pX_{\text{O}} - \left(\frac{3}{2}\right)(p + q)^2 X_{\text{Ba}}X_{\text{O}} - \frac{1}{2}(3q - p)^2 X_{\text{O}}^2 \\
 c_3 &= 1 - \frac{1}{3}(X_{\text{Ti}} + X_{\text{Ba}}) + (p - 1)X_{\text{O}} - \\
 &\quad \left(\frac{1}{3}p + \left(\frac{3}{2}\right)q^2\right)X_{\text{Ti}}X_{\text{O}} - p\left(\frac{1}{3} + \left(\frac{3}{2}\right)p\right)X_{\text{Ba}}X_{\text{O}} - \\
 &\quad p\left(1 + \frac{1}{2}p\right)X_{\text{O}}^2 + \frac{1}{6}(3q - p)^2 X_{\text{Ti}}X_{\text{O}}^2 + \left(\frac{8}{3}\right)p^2 X_{\text{Ba}}X_{\text{O}}^2 + \\
 &\quad \frac{1}{2}(p + q)^2 X_{\text{Ti}}X_{\text{Ba}}X_{\text{O}} \\
 c_4 &= -\frac{1}{3} - \left(\frac{1}{3}p + \left(\frac{3}{2}\right)q^2\right)X_{\text{O}} + \frac{1}{6}(3q - p)^2 X_{\text{O}}^2 + \\
 &\quad \frac{1}{2}(p + q)^2 X_{\text{Ba}}X_{\text{O}} \quad (72)
 \end{aligned}$$

Equation 71 can be reduced to eq 65 when X_{Ti} , X_{Ba} , and X_{O} are all zero. In that case, $c_1 = 0$, $c_2 = c_3 = 1$, and $c_4 = -1/3$, so that the only polarization comes from the ionic displacement of the Ti⁴⁺ ion, X_{Ti} . The free energy of Ti⁴⁺ ions in a nonlinear field will now be considered. Let the

potential energy of a Ti^{4+} ion at position (x,y,z) in the absence of an external field be

$$\Phi(x,y,z) = a(x^2 + y^2 + z^2) + b_1(x^4 + y^4 + z^4) + 2b_2(y^2z^2 + z^2x^2 + x^2y^2) \quad (73)$$

where a = restoring force constant and b_1 and b_2 = nonlinear restoring force constants. They are both positive. Let there be a local electric field, E_{local} , acting on the ion. The additional potential energy is $-q\vec{E}\cdot\vec{r}$, where \vec{r} is the radius vector. Treating this system by statistical mechanics, the partition function, Z , simplified by Stirling's approximation, becomes

$$Z = \left[\left(\frac{e}{Nh^3} \right) (2\pi mkT)^{3/2} \right]^N \left(\int \frac{\exp(-\Phi + q\vec{E}\cdot\vec{r})}{kT} dV \right) \quad (74)$$

The free energy of Ti^{4+} ions, A_E , as a function of temperature, T , and local electric field, E_{local} , is given by the equation

$$A_E = -kT \ln Z \quad (75)$$

However, a free energy, A_p , is more convenient for most purposes, which is analogous to the Gibbs free energy, expressed in terms of the polarization, P , and temperature, T

$$G = A_p = A_E + \vec{E}\cdot\vec{P} \quad (76)$$

with

$$P_i = - \left(\frac{\partial A_E}{\partial E_i} \right)_T \quad (77)$$

Now, eq 76 becomes

$$G = A_E - E_x \left(\frac{\partial A_E}{\partial E_x} \right)_T - E_y \left(\frac{\partial A_E}{\partial E_y} \right)_T - E_z \left(\frac{\partial A_E}{\partial E_z} \right)_T \quad (78)$$

Here, eq 78 is a general expression. The difference between the external field and the local field has not been taken into account yet. Substituting eq 74 into eq 75 and the corresponding results into eq 78, we have

$$G = -NkT \ln \left[\left(\frac{e}{Nh^3} \right) (\pi kT)^3 \left(\frac{2m}{a} \right)^{3/2} \right] + \frac{3N(kT)^2}{4a^2} (3b_1 + 2b_2) + \frac{aP^2}{Nq^2} \left[1 + \frac{kT}{a^2} (3b_1 + 2b_2) \right] + \frac{1}{N^3 q^4} [b_1(P_x^4 + P_y^4 + P_z^4) + 2b_2(P_y^2 P_z^2 + P_z^2 P_x^2 + P_x^2 P_y^2)] \quad (79)$$

Since from eq 69 and eq 79

$$E_{x,\text{local}}^{\text{Ti}} = \left(\frac{\partial G}{\partial P_x} \right)_T = \frac{2aP_{x,\text{Ti}}}{Nq^2} \left[1 + \frac{kT}{a^2} (3b_1 + 2b_2) \right] + \frac{4P_{x,\text{Ti}}}{N^3 q^4} [b_1 P_{x,\text{Ti}}^2 + b_2 (P_{y,\text{Ti}}^2 + P_{z,\text{Ti}}^2)] \quad (80)$$

with P_{Ti} = the polarization arising from ionic displacement of the Ti^{4+} ion, $P_i = \epsilon_0 X_i E_{\text{local}}^i$ where i = species i ,

and the external field, E_x , being applied in the x direction, we get

$$E_{\text{local}}^{\text{Ti}} \epsilon_0 = E_x \epsilon_0 + \left[\frac{1}{3} (P_{\text{Ti}} + P_{\text{Ti}}) + \frac{1}{3} P_{\text{Ba}} + \left(q + \frac{1}{3} \right) P_{\text{O}_a} + \left(-\frac{1}{2}q + \frac{1}{3} \right) (P_{\text{O}_{b1}} + P_{\text{O}_{b2}}) \right] = \frac{2a\epsilon_0 P_{x,\text{Ti}}}{Nq^2} \left[1 + \frac{kT}{a^2} (3b_1 + 2b_2) \right] + \frac{4P_{x,\text{Ti}}}{N^3 q^4} [b_1 P_{x,\text{Ti}}^2 + b_2 (P_{y,\text{Ti}}^2 + P_{z,\text{Ti}}^2)]$$

$$E_{\text{local}}^{\text{Ti}} \epsilon_0 = E_x \epsilon_0 + \left[\frac{1}{3} (P_{\text{Ti}} + P_{\text{Ti}}) + \frac{1}{3} P_{\text{Ba}} + \left(q + \frac{1}{3} \right) P_{\text{O}_a} + \left(-\frac{1}{2}q + \frac{1}{3} \right) (P_{\text{O}_{b1}} + P_{\text{O}_{b2}}) \right] = \frac{P_{x,\text{Ti}}}{X_{\text{Ti}}}$$

$$E_{\text{local}}^{\text{Ba}} \epsilon_0 = E_x \epsilon_0 + \left[\frac{1}{3} (P_{\text{Ti}} + P_{\text{Ti}}) + \frac{1}{3} P_{\text{Ba}} + \left(-p + \frac{1}{3} \right) P_{\text{O}_a} + \left(\frac{1}{2}p + \frac{1}{3} \right) (P_{\text{O}_{b1}} + P_{\text{O}_{b2}}) \right] = \frac{P_{x,\text{Ba}}}{X_{\text{Ba}}}$$

$$E_{\text{local}}^{\text{O}_a} \epsilon_0 = E_x \epsilon_0 + \left[\left(q + \frac{1}{3} \right) (P_{x,\text{Ti}} + P_{x,\text{Ti}}) + \left(-p + \frac{1}{3} \right) P_{x,\text{Ba}} + \frac{1}{3} P_{x,\text{O}_a} + \left(\frac{1}{2}p + \frac{1}{3} \right) (P_{x,\text{O}_{b1}} + P_{x,\text{O}_{b2}}) \right] = \frac{P_{x,\text{O}_a}}{X_{\text{O}_a}}$$

$$E_{\text{local}}^{\text{O}_{b1}} \epsilon_0 = E_x \epsilon_0 + \left[\left(-\frac{1}{2}q + \frac{1}{3} \right) (P_{x,\text{Ti}} + P_{x,\text{Ti}}) + \left(\frac{1}{2}p + \frac{1}{3} \right) P_{x,\text{Ba}} + \left(\frac{1}{2}p + \frac{1}{3} \right) P_{x,\text{O}_a} + \frac{1}{3} P_{x,\text{O}_{b1}} + \left(-p + \frac{1}{3} \right) P_{x,\text{O}_{b2}} \right] = \frac{P_{x,\text{O}_{b1}}}{X_{\text{O}_{b1}}}$$

$$E_{\text{local}}^{\text{O}_{b2}} \epsilon_0 = E_x \epsilon_0 + \left[\left(-\frac{1}{2}q + \frac{1}{3} \right) (P_{x,\text{Ti}} + P_{x,\text{Ti}}) + \left(\frac{1}{2}p + \frac{1}{3} \right) P_{x,\text{Ba}} + \left(\frac{1}{2}p + \frac{1}{3} \right) P_{x,\text{O}_a} + \left(-p + \frac{1}{3} \right) P_{x,\text{O}_{b1}} + \frac{1}{3} P_{x,\text{O}_{b2}} \right] = \frac{P_{x,\text{O}_{b2}}}{X_{\text{O}_{b2}}} \quad (81)$$

By solving all equations in the set of eq 81 except the first for $P_{x,\text{Ti}}$, $P_{x,\text{Ba}}$, P_{x,O_a} , $P_{x,\text{O}_{b1}}$, and $P_{x,\text{O}_{b2}}$ in terms of $P_{x,\text{Ti}}$ and E_x , then when these values are substituted into the first equation of the set (eq 81), an equation which relates E_x and P_{Ti} can be obtained

$$E_x = \frac{c_3}{c_5} \left\{ \frac{2aP_{x,\text{Ti}}}{Nq^2} \left[1 + \frac{kT}{a^2} (3b_1 + 2b_2) \right] + \frac{4P_{x,\text{Ti}}}{N^3 q^4} [b_1 P_{x,\text{Ti}}^2 + b_2 (P_{y,\text{Ti}}^2 + P_{z,\text{Ti}}^2)] \right\} + \frac{c_4}{c_5} \frac{P_{x,\text{Ti}}}{\epsilon_0} \quad (82)$$

with

$$c_5 = 1 + pX_{\text{O}} - \frac{3}{2}p(p+q)X_{\text{Ba}}X_{\text{O}} + \frac{1}{2}p(3q-p)X_{\text{O}}^2 \quad (83)$$

and c_3 and c_4 can be obtained from eq 72. In the

process of setting up eq 81, various polarizations, $P_{x\text{Ba}}$, $P_{x\text{Oa}}$, $P_{x\text{Ob1}}$, and $P_{x\text{Ob2}}$ may be combined into a total polarization P_x which can be further reduced into an equation in terms of $P_{x\text{Ti}}$ only in connection with eq 82

$$P_x = \frac{c_1}{c_5} \epsilon_0 \left\{ \frac{2aP_{x\text{Ti}}}{Nq^2} \left[1 + \frac{kT}{a^2} (3b_1 + 2b_2) \right] + \frac{4P_{x\text{Ti}}}{N^3 q^4} [b_1 P_{x\text{Ti}}^2 + b_2 (P_{y\text{Ti}}^2 + P_{z\text{Ti}}^2)] \right\} + \frac{c_2}{c_5} P_{x\text{Ti}} \quad (84)$$

In the case of spontaneous polarization when $E_x = 0$ but P_x and $P_{x\text{Ti}}$ are not, we may combine with eq 82 and find

$$P_x = \frac{c_5}{c_3} P_{x\text{Ti}} \quad (85)$$

We use eq 84 in connection with eq 82 to express the field in terms of P , rather than P_{Ti} , and find

$$E_x = \frac{c_3}{c_5} \left\{ \frac{2a}{Nq^2} \frac{c_3}{c_5} P_x \left[1 + \frac{kT}{a^2} (3b_1 + 2b_2) \right] + \frac{4}{N^3 q^4} \left(\frac{c_3}{c_5} \right)^2 [b_1 P_x^2 + b_2 (P_y^2 + P_z^2)] \right\} + \frac{c_3 c_4}{c_5^2} \frac{P_x}{\epsilon_0} \quad (86)$$

If we disregard the cubic term, to get the dielectric behavior above T_C , in a small field and solve for P_x , treating the b 's as small quantities, we have

$$P_x = \frac{\frac{Nq^2}{2a} \left(\frac{c_5}{c_3} \right)^2}{\left[1 + \frac{kT}{a^2} (3b_1 + 2b_2) \right]} \left(E_x + \left(-\frac{c_3 c_4}{c_5^2} \right) \frac{P_x}{\epsilon_0} \right) \quad (87)$$

and according to the form of eq 61

$$\alpha = \frac{\frac{q^2}{2a} \left(\frac{c_5}{c_3} \right)^2}{\left[1 + \frac{kT}{a^2} (3b_1 + 2b_2) \right]} \quad (88)$$

Furthermore, eq 86 allows us to integrate because

$$E_x = \left(\frac{\partial G}{\partial P_x} \right)_T \quad (89)$$

Taking into account the first and second terms of eq 79

$$G = -NkT \ln \left[\left(\frac{e}{Nh^3} \right) (\pi kT)^3 \left(\frac{2m}{a} \right)^{3/2} \right] + \frac{3N(kT)^2}{4a^2} (3b_1 + 2b_2) + \left(\frac{c_4}{\epsilon_0 c_5} \right)^2 \left(\frac{Nq^2}{4a^3} \right) k(T - T_0) (3b_1 + 2b_2) P^2 + \left(\frac{c_4}{\epsilon_0 c_5} \right)^4 \left(\frac{Nq^4}{16a^4} \right) [b_1 (P_x^4 + P_y^4 + P_z^4) + 2b_2 (P_y^2 P_z^2 + P_z^2 P_x^2 + P_x^2 P_y^2)] \quad (90)$$

Table 2. Surface Modified Devonshire Theory Using a Core–Shell Model

model	condition	$f_S(P)$ or $F_S(P)$	eq
Zhong et al. ⁶³	surface energy	$\int_S^{1/2} D \delta^{-1} P^2 dS$	97
Shih et al. ³⁶	depolarization energy	$1.7 P^2 (D/L) (d/L)$	98
	multidomain wall energy	$\gamma [(L/D) - 1] (1/L)$	99

Comparing eq 90 with eq 21, we find

$$G_0(T) = -NkT \ln \left[\left(\frac{e}{Nh^3} \right) (\pi kT)^3 \left(\frac{2m}{a} \right)^{3/2} \right] + \frac{3N(kT)^2}{4a^2} (3b_1 + 2b_2) \quad (91)$$

$$\beta = \left(\frac{c_4}{\epsilon_0 c_5} \right)^2 \left(\frac{Nq^2}{4a^3} \right) k(3b_1 + 2b_2) \quad (92)$$

$$-B = \left(\frac{c_4}{\epsilon_0 c_5} \right)^4 \left(\frac{Nq^4}{16a^4} \right) b_1 \quad (93)$$

$$D = \left(\frac{c_4}{\epsilon_0 c_5} \right)^4 \left(\frac{Nq^4}{16a^4} \right) 2b_2 \quad (94)$$

6. Surface-Modified Devonshire Theory

The concept of the core–shell prevails in many theoretical models regarding different geometrical shapes, such as sphere,^{36,62–66} cube,³⁶ cylinder,⁶⁶ and film.⁶⁶ All these models are phenomenological and have an origin of thermodynamics. The free energy density of the ferroelectric, $F(P)$, is first expanded in terms of polarization, P , and then the free energy, $\phi(P)$, is determined by the integration of $F(P)$. The free energy, $\phi(P)$, is actually the sum of the free energy of the core, $\phi_C(P)$, and the free energy of the shell, $\phi_S(P)$

$$\phi(P) = \phi_C(P) + \phi_S(P) \quad (95)$$

Similar to the Devonshire theory,² a more general⁶⁷ Landau–Ginzberg–Devonshire theory⁶⁸ is applied to the free energy of the core, $\phi_C(P)$

$$\phi_C(P) = \int_V \left\{ \frac{A}{2} (T - T_{0,\infty}) P^2 + \frac{B}{4} P^4 + \frac{C}{6} P^6 + \frac{D}{2} (\nabla P)^2 \right\} dV \quad (96)$$

where A , B , C , and $D = \text{constants}$ and $T_{0,\infty} = \text{bulk Curie–Weiss temperature}$. The gradient term $(\nabla P)^2$ accounts for the inhomogeneous distribution of polarization.⁶² The free energy of the surface layer, $\phi_S(P)$, on the other hand, is formulated differently, in accordance with various conditions. They are summarized in Table 2.

The extrapolation length, δ , in eq 97 depends on the intersite interaction as well as the coordinate number within the surface layer.⁶² For a film, this length is independent of film thickness, because the surface coordination number does not change with the film thickness. However, for cylindrical and spherical structures, the coordination number decreases as size decreases, and so the extrapolation length changes with

size. If the extrapolation length at infinite size is δ_f , where the subscript f means film, for a sphere⁶⁶

$$\frac{1}{\delta_S} = \frac{5}{d} + \frac{1}{\delta_f} \quad (100)$$

where the subscript S denotes sphere and d = diameter. For a cylinder⁶⁶

$$\frac{1}{\delta_C} = \frac{5}{2d} + \frac{1}{\delta_f} \quad (101)$$

where the subscript C denotes cylinder. The D , t , and L in eqs 98 and 99 stand for the domain width, the thickness of the Schottky space-charge layer, and the size of the particle, respectively. To reduce the depolarization energy, particles break up into domains of different polarizations. The domain wall energy, γ , is a function of the polarization as well. If there is an external electric field,⁶⁶ the term $-E_{\text{ext}}P$ can be added to eq 96. A slight modification of including x , y , and z components of $(\nabla P)^2$ in eq 96 is also needed if anisotropy is taken into consideration.⁶⁵

In general, by solving the spatial distribution of polarization and substituting the polarization into the free energy expression, the size dependence of T_C may be obtained from the coefficient of the P^2 term in the free energy expression. According to Zhong et al.⁶³

$$T_C = T_{C,\infty} - \frac{6D}{\delta A d} \quad (102)$$

where $T_{C,\infty}$ = the Curie temperature of the bulk crystal, D = constant, A = constant, d = diameter, and δ = the extrapolation length from eq 100 with $\delta_f = 43$ nm. According to Shih et al.³⁶

$$T_C = T_{C,\infty} - \frac{1}{\alpha'} \left[1.7 \frac{Dt}{L^2} + \frac{8c}{3\xi} \right] \quad (103)$$

with

$$\alpha' = \alpha + 3.4 \frac{Dt}{L^2} + \left[-\frac{2\xi}{D}\alpha + \frac{8c}{3\xi} \right] \quad (104)$$

and

$$\xi = \left[\frac{4}{3}c \left(-\alpha - \frac{2}{3}\beta P^2 - \frac{23}{45}\sigma P^4 \right)^{-1} \right]^{1/2} \quad (105)$$

where $T_{C,\infty}$ = the Curie temperature of the bulk crystal, α , β , c = constants, ξ = half-width of the wall, D = domain width, t = thickness of Schottky space-charge layer, and L = size of the particle. Theoretically, if the core-shell model is used, we see that T_C becomes lower as the particle size becomes smaller from eqs 102 and 103.

7. Random Field Theory

Both Devonshire's phenomenological theory² and Slater's local field theory³ are considered as mean field theories. This is because the local electric field, E_{local} ,

in Devonshire's theory is constant at each point in space, and the local electric field of type a (or type I) oxygen, $E_{\text{local}}^{\text{O}_a}$, of type b (or type II) oxygen, $E_{\text{local}}^{\text{O}_b}$, of titanium, $E_{\text{local}}^{\text{Ti}}$, and of barium, $E_{\text{local}}^{\text{Ba}}$, are constants in each unit cell in Slater's theory. However, in a system with defects (impurities and vacancies) randomly distributed over the crystal lattice sites where each defect possesses the electrical moment, a more general approach is required to account for the differences in local electric field from site to site. This approach is called the random field theory.⁶⁹

For simplicity, we will consider dipole orientations in one-dimensional space, and each dipole can be oriented in either a + or a - direction. Let d_i = dipole moment of an atom located at the i th site, d = the magnitude of a dipole, E_i = the random local field which acts on the i th site from the other defects, $\langle d_i \rangle$ = the average of different dipoles on the i th site at the microscopic level, and $D = \overline{\langle d_i \rangle}$ = the observed dipole moment at the macroscopic level. The bar represents spatial averaging and angular brackets thermal averaging.

The Hamiltonian of the system, H , is

$$H = - \sum_i d_i E_i \quad (106)$$

and the local electric field is

$$E_i = \sum_j J_{ij} d_j \quad (107)$$

where J_{ij} = the dipole-dipole interaction. From the Boltzmann principle in statistical thermodynamics, the thermal average of the dipole moment, d , in a field, E , is

$$\langle d \rangle_E = \frac{\text{Tr} \left\{ d_i \exp \left(\frac{d_i E}{kT} \right) \right\}}{\text{Tr} \left\{ \exp \left(\frac{d_i E}{kT} \right) \right\}} \quad (108)$$

where Tr = trace of a matrix, k = Boltzmann's constant, and T = absolute temperature. From the definition of the delta function, $\int dt \phi(t) \delta(t - t_0) = \phi(t_0)$

$$D = \overline{\langle d \rangle_{E_i}} = \int dE \delta(E - E_i) \langle d \rangle_E = \int dE f(E, D) \langle d \rangle_E \quad (109)$$

where $\overline{\delta(E - E_i)} = f(E, D)$, a distribution function of the random field. Equation 109 is a self-consistent equation for macroscopic average dipole moment in terms of D .

Notably, $f(E, D)$ reduces to a delta function in the mean field approximation when we neglect field fluctuation

$$f(E, D) = \overline{\delta(E - E_i)} = \delta(E - \overline{\langle E_i \rangle}) \quad (110)$$

where

$$\overline{\langle E_i \rangle} = \overline{JD} \quad (111)$$

Substituting eq 110 into eq 109, we have

$$D = \int dE \delta(E - \overline{JD}) - \langle d \rangle_E \quad (112)$$

This leads to

$$D = \frac{\text{Tr} \left\{ d_i \exp \left(\frac{d_i \bar{J} D}{kT} \right) \right\}}{\text{Tr} \left\{ \exp \left(\frac{d_i \bar{J} D}{kT} \right) \right\}} \quad (113)$$

Equation 113 is the Weiss mean-field theory⁷⁰ for the order–disorder phase transition. It always has a phase transition at low enough temperature. For a system of only two possible dipole directions, eq 113 reduces to the hyperbolic function

$$D = d \tanh \left(\frac{\bar{J} D}{kT} \right) \quad (114)$$

However, when the fluctuations of the local field become significant, $f(E, D)$ cannot be reduced to the delta function any more. This means that the random field theory for phase transitions is more general than the mean field theory.

In a system with lattice defects, the suppression of ϵ can be explained by eq 109. Lattice defects generally make the distribution function $f(E, D)$ broad. If $f(E, D)$ is too broad, there is no solution of eq 109 for D . The shift of T_C can also be understood by eq 109. Indeed, if $f(E, D)$ is near T_C , $D \rightarrow 0$, and it is valid that

$$f(E, D) = f(E, D=0) + \frac{\partial f}{\partial E} \cdot D \quad (115)$$

Substituting eq 115 into eq 109, and realizing that $f(E, D=0)$ is an even function and symmetrical for a cubic system, we obtain

$$\int dE f(E, D=0) \langle d \rangle_E = 0 \quad (116)$$

and eq 109 reduces to

$$\int dE \frac{\partial f(E)}{\partial E} \langle d \rangle_{E|T_C} = \frac{D}{D} = 1 \quad (117)$$

One can see that eq 117 is in fact an equation for T_C . If the distribution function, $f(E)$, becomes broader and broader, T_C will become smaller and smaller.

8. Summary

Ferroelectric properties of BaTiO₃ include polarization, P , dielectric constant, ϵ , lattice dimensions, a and c , and lattice strains, x and z . The structure–ferroelectricity relationships at different structural levels are summarized in Table 1.

At equilibrium, they can be related to macroscopic properties of temperature, T , electric field, E , and stress, X , by Devonshire's phenomenological theory. T , E , and X are also control parameters for P , ϵ , a , c , x , and z . This approach purely depends on the tertiary structure of BaTiO₃ (ferroelectric domains) by assuming both primary (ionic spacing) and secondary (crystal lattice) structures are perfect. Therefore, the local electric field is constant everywhere.

To link the ferroelectric properties with the primary and the secondary structures, Slater's local field theory provides the connection by computing the exact local

Lorentz field, not assuming spherical symmetry but taking account of the precise crystal structure. The corresponding local electric fields of barium, titanium, and oxygen atoms are the same in each unit cell.

Despite the important role of the primary and secondary structures in ferroelectricity, the Devonshire theory is commonly used in explaining the size effect of BaTiO₃ particles from a quaternary structural point of view. The BaTiO₃ particle is thought to have a ferroelectric core and a paraelectric shell (core–shell model). An extra surface-layer term in the form of either surface energy⁶³ or depolarization energy³⁶ is added to the Devonshire theory to account for the disappearance of ferroelectricity as the particle size is reduced.

The core–shell model does *not* apply to BaTiO₃ particles with defects distributed randomly over the crystal lattice sites. Under this condition, the local electric field fluctuates from site to site. Therefore, the random field theory⁶⁹ is more suitable to describe the disappearance of ferroelectricity; that is, as the distribution function $f(E, D)$ of the random electric field becomes broader and broader, the dielectric constant, ϵ , will be suppressed more and more, and the Curie temperature, T_C , will become smaller and smaller.

Acknowledgment. We gratefully acknowledge support of the Army Research Office (DAL03-92-G-0241 and DAAH04-93-G-0098) and the MRSEC Program Science Foundation (DMR-940032). We thank B. E. Vugmeister for discussing the random field theory with us.

Appendix

- A = constant
- A = coefficient
- A = Helmholtz free energy
- A_0 = free energy of the unpolarized cubic crystal
- A_E = Helmholtz free energy
- A_P = Gibbs free energy
- a = lattice constant
- a = restoring force constant
- a = a axis
- B = constant
- B = coefficient
- $-B$ = coefficient (eq 93)
- Ba = barium atom
- b = lattice constant
- b_1 = nonlinear restoring force constant
- b_2 = nonlinear restoring force constant
- C = constant
- C = coefficient
- C_{11} = average longitudinal elastic constant
- C_{33} = elastic constant
- c = lattice constant
- c_1 = constant
- c_2 = constant
- c_3 = constant
- c_4 = constant
- c_5 = constant (eq 83)
- D = constant
- D = coefficient
- D = coefficient (eq 94)
- D = equilibrium size of the 180° domain
- D = domain width
- D = observed dipole moment at the macroscopic level
- d = equilibrium size of the 90° domain
- d = diameter
- d = magnitude of a dipole
- d_i = dipole moment of an atom located at the i th site

$\langle d_i \rangle$ = average of different dipoles on the i th site at the microscopic level
 E = electric field
 E_0 = field produced by fixed charges external to the body
 E_1 = depolarization field from a surface charge density $\mathbf{n} \cdot \mathbf{P}$ on the outer surface of the specimen (electrodes)
 E_2 = Lorentz cavity field: field from polarization charges on inside of a spherical cavity cut (as a mathematical fiction) out of the specimen with the reference atom as center
 E_3 = field of atoms inside the spherical cavity
 E_{90}^0 = minimum electric field to drive 90° domain spike
 E_{180}^0 = minimum electric field to drive 180° domain spike
 E_C = coercive electric field
 E_{CRTT} = critical electric field
 E_i = the random local field which acts on the i th site from the other defects
 E_{local} = local field acts at the site of the atom
 \vec{E} = electric field vector
 e = electric charge
 F = free energy density
 f = distribution function of the random field
 G = coefficient
 G = elastic Gibbs function
 G_0 = free energy for zero polarization
 G_0 = coefficient (eq 91)
 g = crystal size
 H = Hamiltonian function
 h = Planck's constant
 J = dipole–dipole interaction
 k = Boltzmann constant
 L = size of the crystal
 L = lamina length
 L = size of the particle
 M = domain wall mobility
 m = mass
 N = wall thickness
 N = number of atoms per unit volume
 O = oxygen atom
 O_a = type a oxygen atoms that lie along the same line of the polarization axis
 O_{b1} = first type b oxygen atoms that are at the right angle to the polarization axis
 O_{b2} = second type b oxygen atoms that are at the right angle to the polarization axis
 P = polarization
 P_x = polarization component
 P_y = polarization component
 P_z = polarization component
 \vec{P} = polarization vector
 P_r = remnant polarization
 P_S = spontaneous polarization
 P_{SC} = spontaneous polarization at Curie temperature
 ΔP = discontinuous jump of the spontaneous polarization at Curie temperature upon heating
 ∇P = polarization gradient
 p = pressure (compressive stress)
 p = constant
 Q = cubic–tetragonal phase transition latent heat
 Q_{11} = electrostrictive coefficient
 Q_{12} = electrostrictive coefficient
 Q_{44} = electrostrictive coefficient
 q = constant
 q = charge
 \vec{r} = radius vector
 S = entropy
 S_S = spontaneous strain
 ΔS = cubic–tetragonal phase transition entropy change
 s_{11} = elastic compliance
 s_{12} = elastic compliance
 s_{44} = elastic compliance
 T = temperature
 T_0 = extrapolated temperature of the reciprocal dielectric constant plot

$T_{0,\infty}$ = bulk Curie–Weiss temperature
 T_C = Curie temperature
 $T_{C,\infty}$ = Curie temperature of the bulk crystal
 Ti = titanium atom
 Tr = trace of a matrix
 t = thickness of Schottky space-charge layer
 U = internal energy
 V = forward velocity
 V_{90} = forward velocity of 90° domain spikes induced by the minimum electric field
 V_{180} = forward velocity of 180° domain spikes induced by the minimum electric field
 ΔV = cubic–tetragonal phase transition volume change
 w = lamina width
 X = constant stress
 $X = \alpha/\epsilon_0 v$
 $X' = \alpha'/\epsilon_0 v$
 X_x = normal stress component
 X_y = shear stress component
 X_i = stress component
 x = lattice strain
 $x = x$ direction
 x_i = strain component
 Y_y = normal stress component
 Y_z = shear stress component
 $y = y$ direction
 Z = partition function
 Z_Z = spontaneous strain at room temperature
 Z_z = normal stress component
 Z_x = shear stress component
 $z = z$ direction
 α = constant
 α = electronic polarization
 α = polarizability
 α' = ionic polarization
 α_d = dipolar polarizability
 α_e = electronic polarizability
 α_i = ionic polarizability
 α_s = space charge polarizability
 β = constant
 β = coefficient (eq 92)
 Γ_{90} = 90° domain wall energy
 Γ_{180} = 180° domain wall energy
 δ = extrapolation length
 δ = delta function
 γ = domain wall energy
 γ_S = spontaneous strain
 ϵ = stress
 ϵ = ratio of the permittivity constant of a dielectric material to the permittivity of a free space
 ϵ' = permittivity constant of a dielectric material
 ϵ_0 = permittivity of a free space
 μ = permanent dipole moment
 ξ = half-width of the wall
 σ = domain wall energy
 σ = stress field
 σ^0 = minimum stress
 σ_{anis} = anisotropy
 σ_{dip} = dipole–dipole interaction
 σ_W = total wall energy
 v = the volume of a unit cell
 Φ = potential energy
 ϕ = free energy
 ϕ_C = free energy of the core
 ϕ_S = free energy of the shell
 χ = the susceptibility at constant stress
 $-$ = spatial averaging
 $\langle \rangle$ = thermal averaging

References

- (1) von Hippel, A. R. In *Dielectrics and Waves*; Wiley: New York, 1954; pp 202–213.
- (2) Devonshire, A. F. *Philos. Mag.* **1949**, *42*, 1040–1063.
- (3) Slater, J. C. *Phys. Rev.* **1950**, *78*, 748–761.

- (4) Anliker, M.; Brugger, H. R.; Känzig, W. *Helv. Phys. Acta* **1954**, *27*, 99–124.
- (5) Herczog, A. *J. Am. Ceram. Soc.* **1964**, *47*, 107–115.
- (6) Kiss, K.; Magder, J.; Vukasovich, M. S.; Lockhart, R. J. *J. Am. Ceram. Soc.* **1966**, *49*, 291–295.
- (7) Bachmann, R.; Bärner, K. *Solid State Commun.* **1988**, *68*, 865–869.
- (8) Xu, J. J.; Shaikh, A. S.; Vest, R. W. *IEEE Trans. Ultrason. Ferroelectr. Freq. Control* **1989**, *36*, 307–312.
- (9) Uchino, K.; Sadahaga, E.; Minrose, T. *J. Am. Ceram. Soc.* **1989**, *72*, 1555–1558.
- (10) Vivekanandan, R.; Kutty, T. R. N. *Powder Technol.* **1989**, *57*, 181–192.
- (11) Fujita, T.; Lin, I. J. *Powder Technol.* **1991**, *68*, 235–242.
- (12) Okazaki, K.; Maiwa, H. *Jpn. J. Appl. Phys.* **1992**, *31*, 3113–3116.
- (13) Saegusa, K.; Rhine, W. E.; Bowen, H. K. *J. Am. Ceram. Soc.* **1993**, *76*, 1505–1512.
- (14) Yamamoto, T.; Urabe, K.; Banno, H. *Jpn. J. Appl. Phys. 1* **1993**, *32*, 4272–4276.
- (15) Begg, B. D.; Vance, E. R.; Nowotny, J. *J. Am. Ceram. Soc.* **1994**, *77*, 3186–3192.
- (16) Schlag, S.; Eicke, H. F. *Solid State Commun.* **1994**, *91*, 883–887.
- (17) Schlag, S.; Eicke, H. F.; Mathys, D.; Guggenheim, R. *Langmuir* **1994**, *10*, 3357–3361.
- (18) Yen, F. S.; Hsiang, H. I.; Chang, Y. H. *Jpn. J. Appl. Phys. 1* **1995**, *34*, 6149–6155.
- (19) Zhong, Z.; Gallagher, P. K. *J. Mater. Res.* **1995**, *10*, 945–952.
- (20) Frey, M. H.; Payne, D. A. *Phys. Rev. B* **1996**, *54*, 3158–3168.
- (21) Gotor, F. J.; Real, C.; Dianez, M. J.; Criado, J. M. *J. Solid State Chem.* **1996**, *123*, 301–305.
- (22) Li, X.; Shih, W. H. *J. Am. Ceram. Soc.* **1997**, *80*, 2844–2852.
- (23) Takeuchi, T.; Tabuchi, M.; Ado, K.; Honjo, K.; Nakamura, O.; Kageyama, H.; Suyama, Y.; Ohtori, N.; Nagasawa, M. *J. Mater. Sci.* **1997**, *32*, 4053–4060.
- (24) Bursill, L. A.; Jiang, B.; Peng, J. L.; Ren, T. L.; Zhong, W. L.; Zhang, P. L. *Ferroelectric* **1997**, *191*, 489–494.
- (25) Sakabe, Y.; Wada, N.; Hamaji, Y. *J. Kor. Phys. Soc.* **1998**, *32*, S260–S264.
- (26) McCauley, D.; Newnham, R. E.; Randall, C. A. *J. Am. Ceram. Soc.* **1998**, *81*, 979–987.
- (27) Buessem, W. R.; Cross, L. E.; Goswami, A. K. *J. Am. Ceram. Soc.* **1966**, *49*, 33–39.
- (28) Martirena, H. T.; Burfoot, J. C. *J. Phys. C: Solid State Phys.* **1974**, *7*, 3182–3192.
- (29) Arlt, G.; Hennings, D.; de With, G. *J. Appl. Phys.* **1985**, *58*, 1619–1625.
- (30) Arlt, G.; Pertsev, N. A. *J. Appl. Phys.* **1991**, *70*, 2283–2289.
- (31) Waser, R. *Integr. Ferroelectr.* **1997**, *15*, 39–51.
- (32) Kraševc, V.; Drogenik, M.; Kolar, D. *J. Am. Ceram. Soc.* **1990**, *73*, 856–860.
- (33) Kay, H. F. *Acta Crystallogr.* **1948**, *1*, 229–237.
- (34) Arlt, G.; Sasko, P. *J. Appl. Phys.* **1980**, *51*, 4956–4960.
- (35) Merz, W. J. *Phys. Rev.* **1954**, *95*, 690–698.
- (36) Shih, W. Y.; Shih, W. H.; Aksay, I. A. *Phys. Rev.* **1994**, *B50*, 15575–15585.
- (37) Loge, R. E.; Suo, Z. *Acta Mater.* **1996**, *44*, 3429–3438.
- (38) Matthias, B.; von Hippel, A. *Phys. Rev.* **1948**, *73*, 1378–1384.
- (39) Samara, G. A. *Phys. Rev.* **1966**, *151*, 378–386.
- (40) Shirane, G.; Jona, F.; Pepinsky, R. *Proc. IRE* **1955**, *43*, 1738–1793.
- (41) Kretschmer, R.; Binder, K. *Phys. Rev.* **1979**, *20*, 1065–1076.
- (42) Merz, W. J. *Phys. Rev.* **1953**, *91*, 513–517.
- (43) Fatuzzo, E.; Merz, W. J. In *Selected Topics in Solid State Physics*; Wohlfarth, E. P., Ed.; Wiley: New York, 1967; Vol. VII (Ferroelectricity); pp 105–147.
- (44) Vivekanandan, R.; Kutty, T. R. N. *Powder Technol.* **1989**, *57*, 181–192.
- (45) Murugaraj, P.; Kutty, T. R. N.; Subba Rao, M. *J. Mater. Sci.* **1986**, *21*, 3521–3527.
- (46) Hsiang, H. I.; Yen, F. S. *Jpn. J. Appl. Phys. Part 1* **1993**, *32*, 5029.
- (47) Merz, W. J. *Phys. Rev.* **1949**, *76*, 1221–1225.
- (48) Kingery, W. D.; Bowen, H. K.; Uhlmann, D. R. In *Introduction to Ceramics*, 2nd ed.; Wiley: New York, 1976; pp 964–973.
- (49) Kittel, C. In *Introduction to Solid State Physics*, 6th ed.; Wiley: New York, 1986; pp 360–394.
- (50) Remeika, J. P. *J. Am. Chem. Soc.* **1954**, *76*, 940–941.
- (51) Zhu, W.; Wang, C. C.; Akbar, S. A.; Asiaie, R. *J. Mater. Sci.* **1997**, *32*, 4303–4307.
- (52) Forsbergh, P. W., Jr. *Phys. Rev.* **1949**, *76*, 1187–1201.
- (53) Harwood, M. G.; Popper, P.; Rushman, D. F. *Nature* **1947**, *160*, 58–59.
- (54) Kay, H. F.; Vousden, P. *Philos. Mag.* **1949**, *7*, 1019–1040.
- (55) Fatuzzo, E.; Merz, W. J. In *Selected Topics in Solid State Physics*; Wohlfarth, E. P., Ed.; Wiley: New York, 1967; Vol. VII (Ferroelectricity), pp 171–189.
- (56) von Hippel, A. R. In *Dielectric Materials and Applications*; Wiley: New York, 1954; p 20.
- (57) Chiou, B. S.; Lin, S. T.; Duh, J. G.; Chang, P. H. *J. Am. Ceram. Soc.* **1989**, *72*, 1967–1975.
- (58) von Hippel, A. R. In *Dielectrics and Waves*; Wiley: New York, 1954; pp 30–36.
- (59) von Hippel, A. R. In *Dielectrics and Waves*; Wiley: New York, 1954; pp 36–40.
- (60) Onsager, L. *J. Am. Chem. Soc.* **1936**, *58*, 1486–1493.
- (61) Kirkwood, J. G. *J. Chem. Phys.* **1939**, *7*, 911–919.
- (62) Wang, J. G.; Zhong, W. L.; Zhang, P. L. *Solid State Commun.* **1994**, *92*, 519–523.
- (63) Zhong, W. L.; Wang, Y. G.; Zhang, P. L.; Qu, B. D. *Phys. Rev.* **1994**, *B50*, 698–703.
- (64) Li, S.; Eastman, J. A.; Li, Z.; Foster, C. M.; Newnham, R. E.; Cross, L. E. *Phys. Lett. A* **1996**, *212*, 341–346.
- (65) Li, S.; Eastman, J. A.; Vetrone, J. M.; Foster, C. M.; Newnham, R. E.; Cross, L. E. *Jpn. J. Appl. Phys. Part 1* **1997**, *36*, 5169–5174.
- (66) Wang, C. L.; Smith, S. R. P. *J. Phys.: Condens. Matter* **1995**, *7*, 7163–7171.
- (67) Ginzberg, V. L. *Ferroelectrics* **1987**, *76*, 3–22.
- (68) Ginzberg, V. L.; Levanyuk, A. P.; Sobyamin, A. A. *Ferroelectrics* **1987**, *73*, 171–182.
- (69) Vugmeister, B. E.; Glinchuk, M. D. *Rev. Mod. Phys.* **1990**, *62*, 993–1026.
- (70) Lines, M. E.; Glass, A. M. In *Principles and Applications of Ferroelectrics and Related Materials*; Clarendon Press: Oxford, U.K., 1977; pp 24–58.